ADVANCED PAPERMAKING INITIATIVE

2023

THE UNIVERSITY OF BRITISH COLUMBIA

WELCOME MESSAGE

Dear reader:

This latest report encapsulates the significant advances we have made in the past year and provide a profound understanding of our investigations.

We would also like to extend our appreciation to our colleague and dear friend Dr. Richard Kerekes for his induction into the prestigious 2023 Chemical and Biological Engineering Hall of Fame at UBC. This recognition is a testament to his exceptional contributions to the UBC Pulp and Paper Centre, the university as a whole, and the field of chemical and biological engineering. I encourage you to turn to page 38, where you will find a more detailed description of this award and Dick's achievements.

Sincerely,

Mark Martinez

Mark Martinez, Ph.D., P. Eng.,
Professor of Chemical and Biological Engineering, UBC
Principal Investigator, ERMP Research Program

CONTRIBUTORS

Nilgun Abali
Matthias Aigner
Rodger Beatson
Sam Brown
Michael Bilek
Siwei Chen
Emily Cranston
Salman Dajani
James Drummond
Elisa Ferreira
Mariana Frias de Albuquerque
Vijay Kumar Pediredla
Runxin Lai
Stephen Lee
Juliana Lima de Freitas
Mark Martinez
Lewis Mason
Gloria Noki
James Olson
André Phillion
Scott Renneckar
Norman Roberts
Farah Sadek
Laurel Schafer
Boris Stoeber
Heather Trajano
Nicole Ting
Daniela Vargas Figueroa
Anderson Veiga
Peter Wild
Adam Wu
Fariba Yeganeh
Cameron Zheng

DESIGNER CONTACT
Program Manager
Daniela Vargas Figueroa
daniela.figueroa@ubc.ca
604-827-2390

UBC Pulp and Paper Centre
2385 East Mall Vancouver, BC V6T 1Z4

CONTENTS

RESEARCH UPDATES

System design, Sensors and Control

4 **PROJECT 1.1** - LC refining of mechanical pulp. Matthias Aigner, Samira Gharehkhani, Terri Lacourse, Mark Martinez, James Olson, Peter Wild. UVic and UBC

9 **PROJECT 1.2** - Deep-learning based control and optimization in the thermomechanical pulping process. Vijay Kumar Pediredla, Bhushan Gopaluni, Yankai Cao. UBC

13 **PROJECT 1.3** - Creating low-energy shive-free pulps. Claire Maulit, Rodger Beatson, Heather Trajano, Gloria Noki, Renz Po, Runxin Lai. BCIT & UBC

Valorization of TMP fines

18 **PROJECT 2.1** - Lignin-rich fines: Simple routes towards creation of hydrophobic and hydrophilic filler additives. Scott Renneckar, Siwei Chen, Adam Wu. UBC

24 **PROJECT 2.2** - From trees to treatment: Functionalizing TMP extractives. Cameron Zheng, Juliana Lima de Freitas, Laurel Schafer, Heather Trajano. UBC

27 **PROJECT 2.3** - MFC production, characterization, and properties from mechanical pulps. Mariana Frias de Albuquerque, James Olson, Heather Trajano, Boris Stoeber, UBC

New Product Development

31 **PROJECT 3.1** - Creating bulky fibres. Elisa Ferreira, Jason Sugiharto, Anderson Veiga, Emily Cranston, Mark Martinez, UBC

33 **PROJECT 3.2** - Advanced characterization: Computed tomography. Aurélien Sibellas, James Drummond, Sam Brown, Lewis Mason, André Phillion, Elisa Ferreira, Anderson de Veiga, Emily Cranston, Mark Martinez. McMaster & UBC

PROGRAM UPDATES

35 **ERMP Personnel Updates**

38 **PPC Highlights**

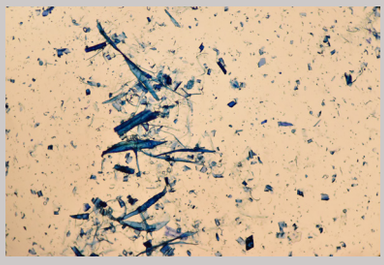

ON THE COVER

On the cover, a light microscopy image of unfractionated microfibrillated cellulose fibres stained with toluidine blue. **Author: Michael Bilek, Research Assistant.**

PROJECT 1.1

LC REFINING OF MECHANICAL PULP

Authors: Matthias Aigner, Samira Gharehkhani, Terri Lacourse, Mark Martinez, James Olson, Peter Wild

Background

In previous work by researchers at the University of Victoria, a custom piezo-ceramic force sensor was developed to measure local shear and normal forces applied to the refiner bars. Sensors based on this design have been used in trials in a variety of high consistency (HC) [Olender et al. 2008] and low consistency (LC) [Harirforoush et al. 2018] refiners. Most recently, trials were conducted at the Pulp and Paper Centre at UBC and at the Catalyst, Paper Excellence mill in Crofton, BC [Aigner et al. 2020, Aigner et al. 2022]. The goal of these studies was to investigate the effect of operating conditions on the radial distributions of bar-force, as characterized by the force profile during bar-passing events. From this work, new research questions emerged such as the impact of rotational speed and bar width on the refining process.

Trial set up

To expand on the previous findings of this research group, a comprehensive set of experiments was designed for and performed on the 16-inch AIKAWA single disc refiner at the PPC. The goal of these experiments is to investigate the effect of refiner plate geometry, such as bar width and bar edge length (BEL), and refining parameters, such as specific edge load (SEL) and rotational speed, on bar force profiles and fiber and paper properties. The complete set of trials is intended to be a baseline study with potential to extend the knowledge of LC refining of mechanical pulp and aid in the development of new refiner plate designs.

The study is made up of three refiner plates run at two rotational speeds and three different SEL each, which results in a total of 18 trials. Table 1 presents a summary of the trials. Note that Plates 1 and 2 have the same bar width while Plates 1 and 3 have the same BEL. This allows to investigate the impact of bar width and BEL on the refining process. These trails were completed in summer 2022.

Each trial is run in recirculation mode and fiber samples are taken at the no load position (S0) and at five times throughout each the trial (S1-S5), with approximately equal accumulated Specific Refining Energy (SRE) between samples. Similar to our previous work, a sensor and a rotary encoder were installed on the refiner to record the bar forces and reference these to the position of the rotor with respect to the bar force sensor. The force sensor and encoder sample continuously throughout each trial.

Table 1. Summary of the operating conditions for the pilot-scale LC refining trials.

	Plate 1 BEL: 2.1 km/rev Bar width: 1.4 mm	Plate 2 BEL: 5.4 km/rev Bar width: 1.4 mm	Plate 3 BEL: 2.1 km/rev Bar width: 2.5 mm
	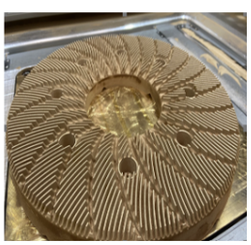		
Rotational speed (rpm)	1200, 1600	1200, 1600	1200, 1600
SEL (J/m)	0.2, 0.4, 0.8	0.1, 0.2, 0.3	0.2, 0.4, 0.8
Consistency (%)	3.5	3.5	3.5
Flow rate (L/m)	250	250	250
Pulp type	Mechanical softwood pulp, Initial freeness 500 CFI, initial fiber length 1.45mm		

PROJECT 1.1

Results

Trials completed and analysis

Trial data are analysed with multivariate analysis using Principal Component Analysis (PCA) followed by Redundancy Analysis (RDA). Summary results are shown in Figure 1. Input and output variables with their respective loadings are listed in Table 2.

As shown in Figure 1 (a), data points group together based on the sample (i.e. S0, S1, S2 etc.) from which they are drawn. The PCA shows that 68.32% of the variation in the data can be explained by the first principal component (PC1) while 11.61% of the variation is explained by PC2. This indicates that two-thirds of the variation in the trial data is explained by PC1.

Considering the loadings of the output variables, shown as vectors in Figure 1 (b), the variables which are maximally opposed and contribute the most to PC1 are accumulated SRE, on one hand, and freeness and fiber length, on the other. For example, data points at the negative end of the scatter plot shown in Figure 1 (a) are earlier in their respective trials (i.e., S0 or S1), have lower accumulated SRE, greater fiber length and higher freeness.

Considering now the loadings of the output variables in the PC2 dimension, shown in Figure 1 (b), the maximally opposed variables are mean shear/normal force and accumulated SRE. This indicates that for increasing accumulated SRE, the measured normal and shear forces decrease.

The loadings for the input variables, as determined by the RDA, are shown in Figure 1 (c). Variance for RDA 1 are 41.42 % and for RDA 2, 3.8% For the RDA 1 dimension, the loadings of gross power and gap are opposed.

For the RDA 2 dimension the loadings of the input variables are low compared to the PDA 2 dimension and gap and BEL are the opposed variables.

When comparing the input variable loadings, shown in Figure 1 (c), to the loadings of the output variables, shown in Figure 1 (b), the input variable, gap, plots in the same direction as the output variable, freeness, while the input variable, gross power, plots in the same direction as the output variable, accumulated SRE. For the PC2 dimension, comparing loadings for input and output variables, the input variable, gap, aligns with the output variable, accumulated SRE, and the input variable, BEL, aligns with the output variables, normal force and shear force.

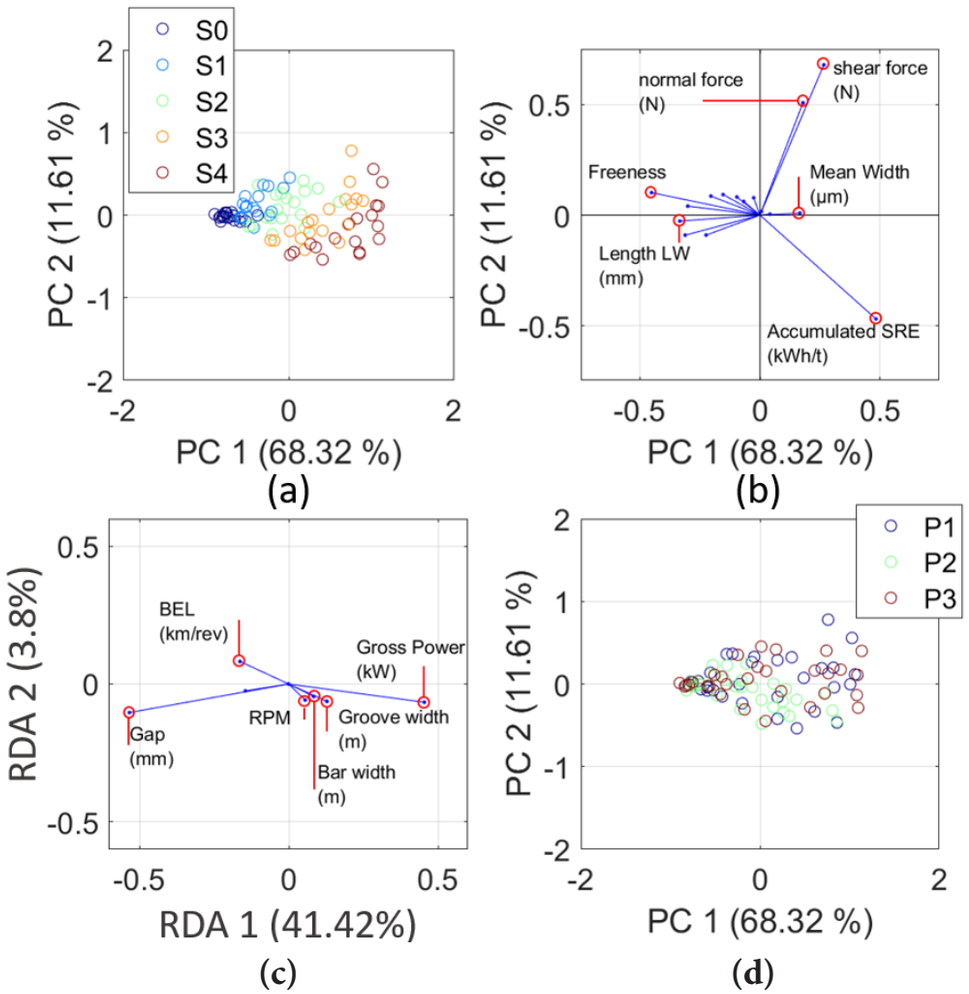

Figure 1. PCA analysis of all 18 trials for sample points S0-S4. (a) Scatter plot of all data points in PC1 and PC2, colour coded based on sample points. (b) Loading of all output variables in PC1 and PC2. (c) Loading of all input variables in PC1 and PC2 (d) Scatter plot of all data points in PC1 and PC2, colour coded based the plate used.

PROJECT 1.1

Table 2. Output and input variables used in the RDA and the PCA and their respective loadings in PC1 and PC2 dimension. The extreme values are highlighted in bold.

Output variables			Input variables		
	68.32%	11.61%		41.42%	3.80%
	PC1	PC2		RDA 1	RDA 2
	Loadings			Loadings	
Fines Arithmetic (LN)	0.04	0.00	Gross Power (kW)	**0.45**	-0.06
Fine Percentage LW(%)	0.17	0.01	RPM	0.04	-0.05
Length Arithmetic (LN)	-0.22	-0.09	Flow (L/min)	-0.16	-0.02
Length LW (mm)	**-0.33**	-0.03	Gap (mm)	**-0.55**	**-0.10**
Length WW (mm)	-0.31	-0.09	Bar width (m)	0.09	-0.05
Curl Index Arithmetic (LN)	-0.07	0.06	Groove width (m)	0.11	-0.06
Curl Index LW (mm)	-0.10	0.08	BEL (km/rev)	-0.15	**0.09**
Kink Index (1/mm)	-0.20	0.09			
Total Kink angle (°)	-0.30	0.04			
Kinks per mm	-0.15	0.09			
Mean Width (µm)	0.01	0.02			
Freeness	**-0.45**	0.10			
mean shear force (N)	0.27	**0.68**			
mean normal force (N)	0.18	**0.51**			
Consistencies (%)	-0.03	0.08			
Accumulated SRE (kWh/t)	**0.48**	**-0.47**			

Figure 1 (d) is a variation of Figure 1 (a) with the data points colour coded to indicate the plate used. The spread of the data in PC1 direction is comparable for all plates. This indicates that accumulated SRE and fiber length (Length LW) behave comparably among the plates. This also indicates that the gross power and gap behave mostly comparable between the plates. In PC2 direction, Plate 1 and Plate 3 draw more into the top right quadrant of the plot in Figure 1 (d). This indicates that these data points have different behaviours in this dimension. For the output variables this indicates that the measured force (mean normal force and mean shear force) and SRE behaviour differs for Plate 2 from Plate 1 and 3. For the input variable in PC2 direction we have gap and BEL opposed. As Plate 1 and Plate 3 share the same BEL which is smaller than Plate 2, the PC 2 direction indicates that Plate 2 refines at a smaller gap.

To sum up the PCA analysis, in PC1 direction, which accounts for the majority of the variation between the data points, trends in the output variables are visible that are expected. For example, decreasing fiber length and freeness with increasing accumulated SRE is reasonable. In looking at the next principal component dimension, PC2, an additional relationship can be seen. Specifically, this dimension indicates that lower normal and shear forces occur with increasing accumulated SRE.

Adding the input variables in form of the RDA, suggests in the PC1 dimension again expected trends. For example, a smaller gap is needed at higher accumulated SRE, and higher power leads to lower freeness and fiber length. Looking at the PC2 dimension also shows expected trends. One is that a smaller gap results in higher forces. An interesting trend is that higher accumulated SRE occurs for plates with lower BEL.

The presented analysis was conducted to better manage and understand this multidimensional and multifaceted data set. Through understanding the results gathered in these trials, the authors goal is to produce a unifying prediction model for trials of this type.

PROJECT 1.1

Force analysis and power prediction

A model to predict the power expended on the pulp fibers based on the measured forces is in development. Using images of the rotor and stator plates (Figure 2 (a), (b)), overlap areas between stator and rotor bars during refining are identified, measured and catalogued, as done previously by Elahimehr et. al. [Elahimehr et al., 2012]. Using the overlap areas, A_i, (Figure 2 (c)), radial position of these areas, r_i, (Figure 2 (d)), rotational speed, ω, and the shear stress based on force sensor measurements, σ, an estimate of the expended power, P, can be made for each contact area. From there the total power for the whole number of contacts, N_c, can be determined as described in Equation 1.

$$P = \sum_{i=1}^{N_c} \sigma A_i r_i \omega \qquad (1)$$

The power calculated this way for the recent trials with plates from Valmet are plotted versus the gross power measured during these trials in Figure 3. Plate 1, shown in Figure 3 (a), shows a linear trend for the data for the 1200 rpm trials. The estimate for the 1600 rpm trials varies significantly. For Plate 2 the 1200 rpm estimates are greatly over estimating the measured gross power while the 1600 rpm data increases in approximate accordance with the measured gross power although the estimate under estimates the measured gross power. For plate 3 the calculation underestimates the measured gross power for both 1200 and 1600 rpm trials but the progression is very much in line with the measurements.

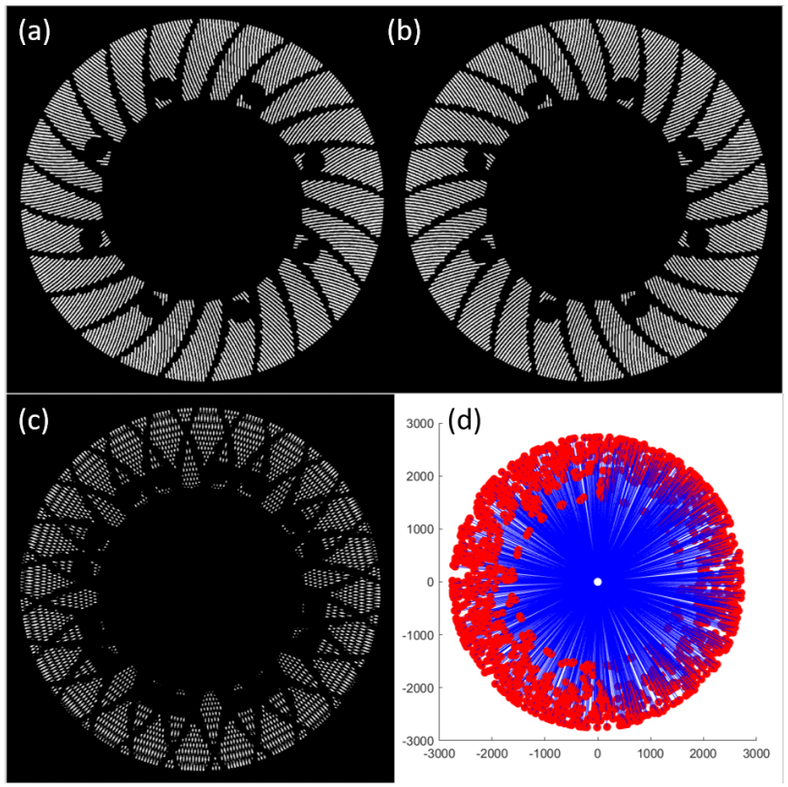

Figure 2. Refiner plate analysis using Valmet plates. Converted black and white file of rotor (a) and stator (b) side by side, (c) overlap areas, (d) centroids and radii for each overlap area.

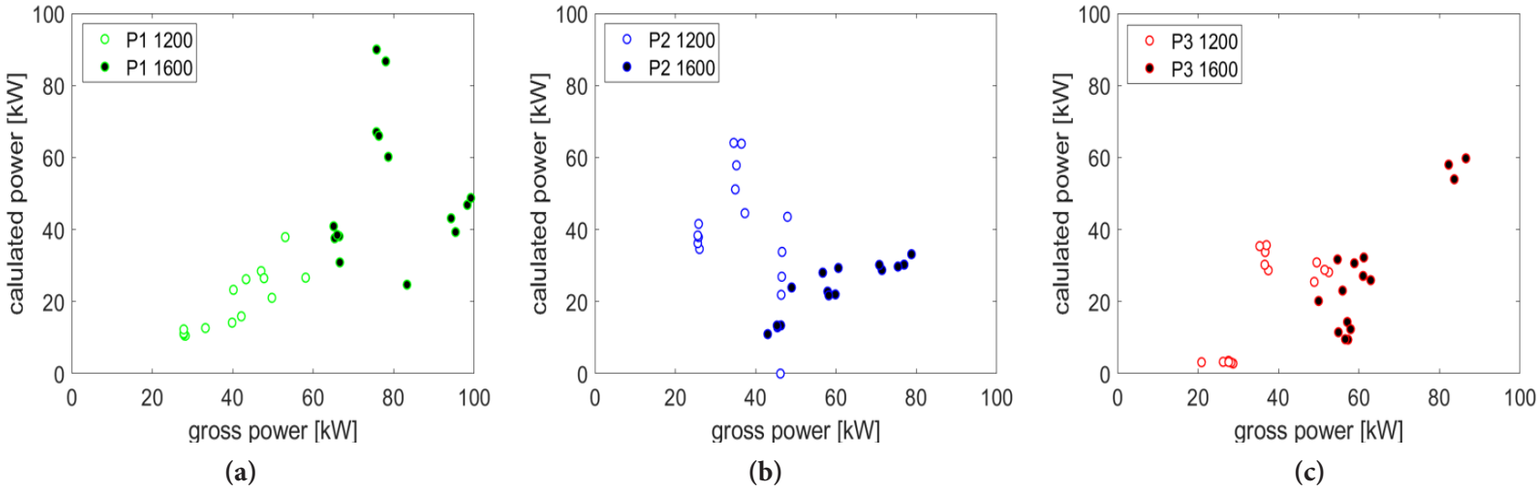

Figure 3. Power calculated based on force measurements for (a) plate 1, (b) plate 2 and (c) plate 3

PROJECT 1.1

Force analysis and power prediction (cont.)

Calculated power for all three plates is plotted together in Figure 4. For data point for Plates 1 and 3 at 1200 and 1600 rpm and Plate 2 at 1600 rpm the calculation underestimates the measured gross power. In total the calculation underestimates the gross power for 88% of data points (Figure 4 (b)). Calculated power for Plate 2 at 1200 rpm overestimates the power expended.

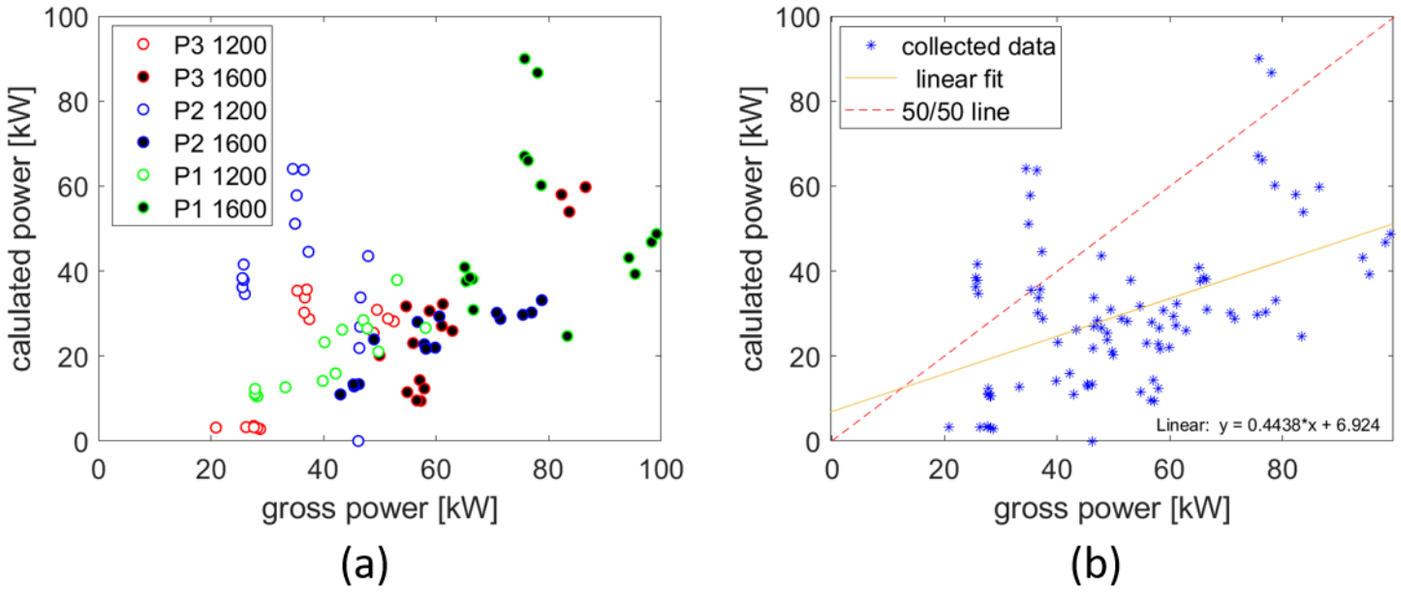

Figure 4. (a)Power calculation plotted against gross power for all plates (b) including trend line and 50/50 line.

Acknowledgements

The authors thank Mr. Norm Roberts for conducting the refining trials and the co-op students at the UBC-PPC for their hard work in analysing the fibre data.

References

1. Aigner, M., Olson, J., and Wild, P. (2020). Measurement and interpretation of spatially registered bar-forces in LC refining. Nordic Pulp & Paper Research Journal, 35(4), 600-610.
2. Aigner, M., Olson, J., Sun, Y., and Wild, P. (2022). Interpretation of force profiles in mill-scale LC refining. Nordic Pulp & Paper Research Journal, 37(1), 42-53.
3. Harirforoush, R, Olson, J., and Wild, P. (2017). In-Process Detection of Fiber Cutting in Low Consistency Refining Based on Measurement of Forces on Refiner Bars. Tappi Journal 16 (4): 460–69.
4. lender, D., Wild, P., & Byrnes, P. (2008). A piezoelectric force sensor for mill-scale chip refiners. Proceedings of the Institution of Mechanical Engineers, Part E: Journal of Process Mechanical Engineering, 222(2), 115-122.
5. Elahimehr, A.;Martinez, D.M.;Olson, J. A. (2012): A Method For Estimating the Area of Intersection Between Refiner Plates. J. Powder Technol., (February 2012), 1–18.

PROJECT 1.2

DEEP-LEARNING-BASED CONTROL AND OPTIMIZATION IN THE THERMOMECHANICAL PULPING PROCESS

Authors: Vijay Kumar Pediredla, Bhushan Gopaluni, Yankai Cao

Background

Thermomechanical pulping (TMP) processes are widely used for newsprint productions owing to their relatively high pulp yield. However, the mechanical pulping process is also highly energy intensive, and the pulp and paper industry is ranked fourth among all industries in total greenhouse gas emissions. Due to the increase in electricity prices, environmental concerns, and low energy efficiency, the research focuses on energy consumption optimization while maintaining the expected pulp quality. Various methodologies have been developed to address the energy reduction objective, where the multivariate process control strategies and real-time optimization (RTO) methods [1] were most prevalent. Typical examples of advanced process control are the different model predictive control (MPC) techniques developed to regulate the TMP processes addressing its dynamic and complex nature. Multi-objective economic MPC strategies with state estimation are proposed to address the trade-off between economic and setpoint tracking performance [2]. Other proposed MPC approaches are the simplified linear MPC strategy, the generalized predictive controller, and the inferential MPC design. Moreover, well-designed offset-free MPC strategies have been employed to address model uncertainty and process disturbance. However, these are based on assumptions, and there is also a risk of fiber cutting and, eventually, a plate clash. Understanding the effect of the pulping process operating conditions on the fibrous structure of the final product would enable the manufacture of the paper with desired properties.

Artificial Intelligence (AI) and Machine-Learning (ML) developments have presented new opportunities for industries to capitalize on these emerging technologies. The pulp and paper industries are undergoing one of the most considerable transformations into Industry 4.0. Integrating AI technology in the manufacturing process of the pulp and paper industry has shown great potential for process automation, energy efficiency, and decision-making. For example, images from 3D X-ray tomography are used in conjunction with advanced deep learning-based image processing techniques to correlate the fibre microstructure in paper handsheets.

Summary of the work done

Process Operation Evaluation and Model Reliability Assessment for Pulping Process

In the continuous TMP process, aiming at improving energy efficiency and maintaining the produced pulp quality, a non-intrusive operating recommendation system is proposed with an extensible framework. This system uses a high-dimensional visualization technique based on the Kiviat diagram to integrate the multi-dimensional process operating space and the product quality. Simple and robust model structures are employed with sufficient accuracy, and intuitive illustrations of the process operating conditions with comprehensible statistics are provided for real-time implementation. The proposed work links the process operating space to the intermediate pulp properties, controlled to regulate the handsheet properties, as shown in Figure 1 (a). To further investigate the relationship between pulp properties and the handsheet properties, an inferential sensor model was developed with a reliability index to indicate which input sample area is more likely to provide more accurate predictions.

Deep learning-based hybrid reconstruction algorithm for fibre segmentation from 3D X-ray images

3D X-ray tomography is a powerful scanning technique for generating images of complex fibre structures. A novel machine-learning algorithm to identify and separate individual fibres using 3D images is proposed in this article. The developed four-step hybrid 3D fibre segmentation algorithm involves deep-learning aided semantic segmentation that slices 3D images to create 2D images for fibre extraction, elliptical contour estimation combined with the marker-controlled watershed algorithm for separating fibres, identifying individual fibres through 3D reconstruction, and lastly, the 3D object refining approach, as shown in Figure 1 (b). The proposed methodology is implemented on a real-time sample of nylon fibre bundle under compression and its 3D X-ray image volume to validate the performance. The results show its superior performance compared to off-the-shelf image processing algorithms in terms of precision, with a validation accuracy greater than 90% and efficiency, preventing the need for a huge data set and reducing the complexity.

PROJECT 1.2

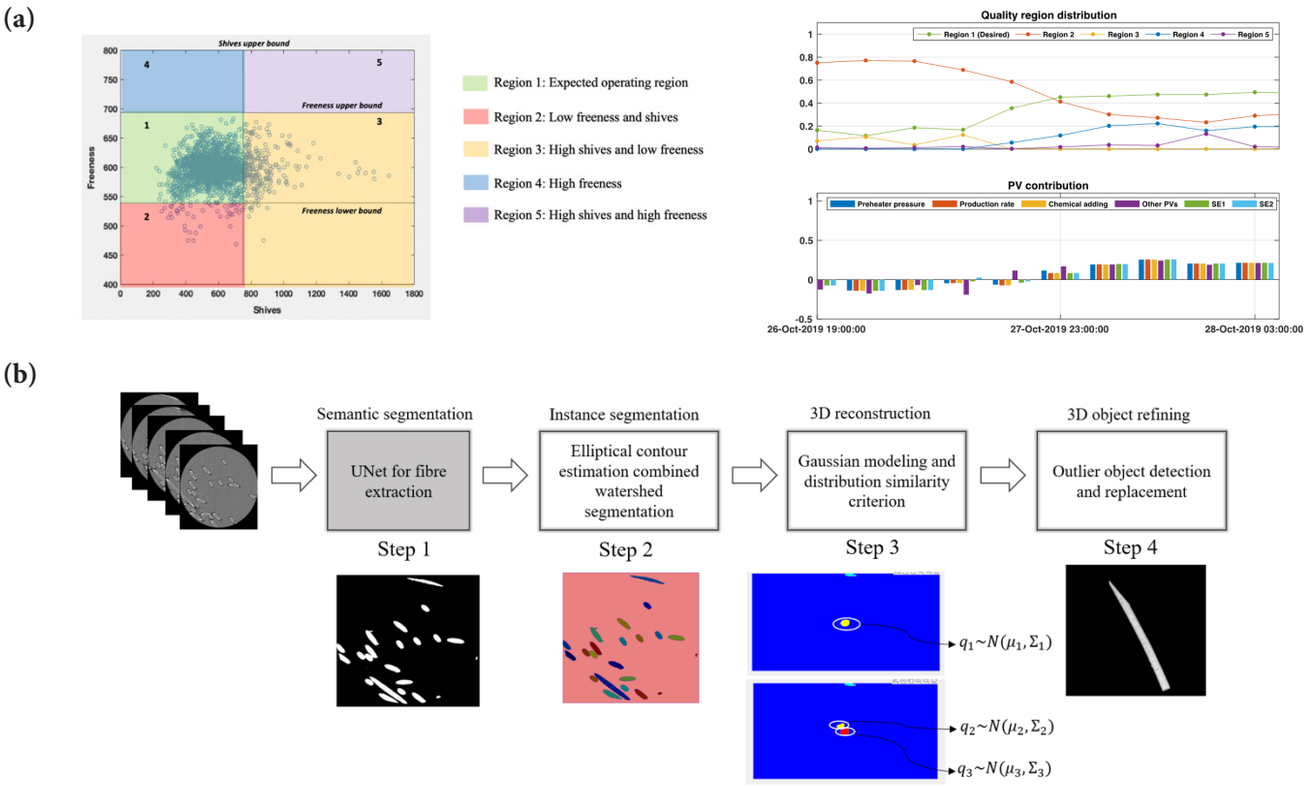

Figure 1. (a) Pulp property segmentation and process variable contribution indices. (b) Workflow of the deep-learning-based hybrid reconstruction algorithm for fibre segmentation

Deep learning-based Model Predictive Control

Model predictive control (MPC) utilizes an explicit process model to compute a sequence of manipulated variables that optimizes the objective function subject to various constraints. MPC is an attractive solution for applications like process industries, automobiles, robotics, aerospace, etc. The primary advantages of using this methodology are the resiliency against uncertainties and disturbances and accommodating constraints. However, the challenges for better performance of MPC are the model mismatch and high computational efforts, especially for complex nonlinear systems. Combining machine learning algorithms with the MPC would augment the performance by addressing the abovementioned challenges.

Machine learning addresses the challenges by collecting large data, utilizing faster computers, and using better measurement techniques. The application of AI and ML in manufacturing is still either in the preliminary analysis stage or laboratory experiments. Some issues in the paper industry, such as paper breakage, have been addressed by integrating sensor data with machine-learning techniques to design predictive models that estimate the breakage time in the system [3]. There have also been developments in predictive maintenance, including sensor exploration, system maintenance, and inspection.

In this methodology, the challenges with physics-based modeling and black-box modeling for predictive control are addressed by combining both these techniques. The dynamic behavior of the output variables and system disturbances are also captured. The order of auto-regression denoted by $\delta_{\{y,w,u\}}$ are hyperparameters chosen during cross-validation. In the learning step, y, w, and u time series were structured from raw sensor data to create data samples at each time instance. Deep neural networks are used for learning complex models with the adaptive updating laws for the weight parameters, as shown in Figure 2.

PROJECT 1.2

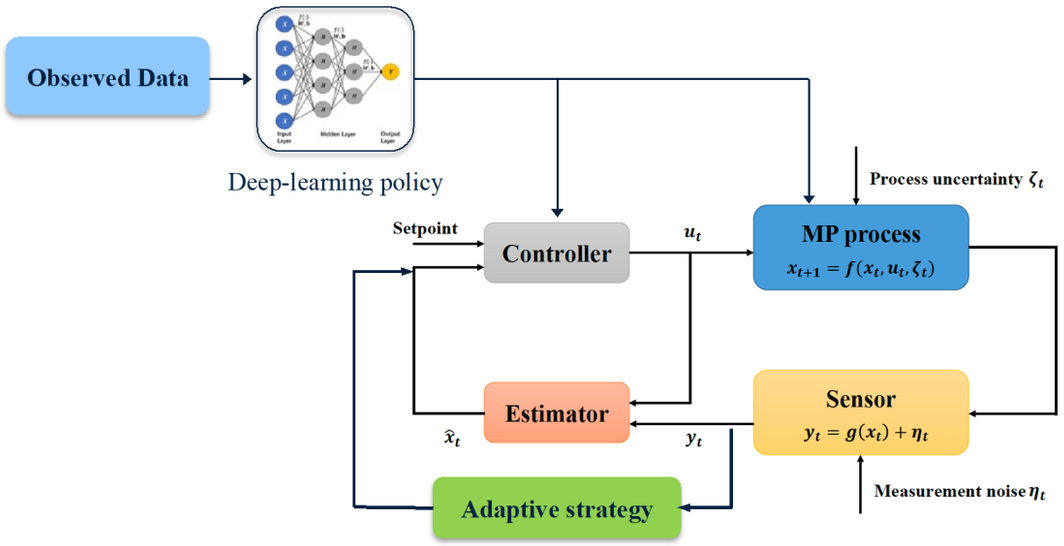

Figure 2. Adaptive deep-learning-based Model Predictive Control.

The optimal control problem is defined as follows:

$$\text{minimize} \quad \underset{u_0,\dots,u_{N-1}}{} \sum_{t=0}^{N-1} W_i(y_{t+1} - y_{\text{ref}})^2 + u_t^T R u_t$$

subject to

$$y_{t+1} = f\left(y_t, y_{t-1}, \dots, y_{t-\delta_y}, w_t, w_{t-1}, \dots, w_{t-\delta_w}, u_t, u_{t-1}, \dots, u_{t-\delta_u}\right), u_t \in \mathcal{U}$$
$$\forall t \in \{0, \dots, N-1\}$$

$$\dot{\hat{W}}_i = P_i[\varphi_i(y_i)^T + \varphi_{if}^T e_{if} + k_i H_{if} \tilde{W}_i)]$$

where u is the control input, w represents disturbances, N is the control horizon, R is the cost matrix, $W_i \in R^{nixn}$ is the weight matrix with n_i nodes, y_{ref} is the reference to be tracked, k_i is the convergence rate gain, e is the error, H_{if} is the admissible initial states, and P_i are the positive definite learning matrices.

Preliminary results

The proposed adaptive deep-learning based MPC is developed for the high-consistency TMP process to demonstrate the energy cost reduction compared to the existing methods while ensuring closed-loop stability and convergence. It is assumed that all the variables in the MP process are measurable. In Figure 3 (a), the tracking performance has been achieved adequately for primary consistency. For the secondary consistency, a constraint has been imposed at 50%, and from Figure 3 (a), it is clear that the proposed method could satisfy the constraints and still track the setpoint. Figure 3 (b) compares the energy savings using the deep-learning MPC with the standard MPC.

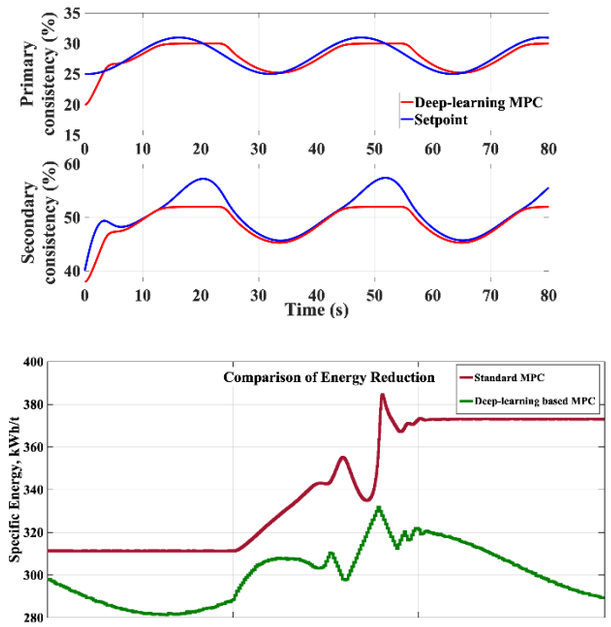

Figure 3. (a) State variables of the TMP process by using deep-learning MPC (b) Comparison of energy reductions.

PROJECT 1.2

Conclusions and Future Work

A deep-learning-based adaptive MPC has been developed, and some preliminary experiments have been performed on the high-consistency TMP process. To further improve the proposed method and to implement it in the present paper and pulp industry, the following steps are taken:

- Discussing current issues and potential solutions that can be implemented practically.
- Collecting data for accurate modeling of the process and performing simulations.
- Prospects of implementing advanced controllers/data-analytics algorithms into the present paper and pulp industrial set-up.

References

1. Hui Tian, Qiugang Lu, R Bhushan Gopaluni, Victor M Zavala, and James A Olson. An economic model predictive control framework for mechanical pulping processes. Control Engineering Practice, 85:100–109, 2019.
2. Eranda Harinath, LT Biegler, and Guy A Dumont. Predictive optimal control for thermo-mechanical pulping processes with multi-stage low-consistency refining. Journal of Process Control, 23(7):1001–1011, 2013.
3. Bonissone, P., Goebel, K., & Chen, Y. T. (2002). Predicting wet-end web breakage in paper mills. In Working Notes of the 2002 AAAI symposium: Information Refinement and Revision for Decision Making: Modeling for Diagnostics, Prognostics, and Prediction (pp. 84-92).

PROJECT 1.3

CREATING LOW-ENERGY SHIVE-FREE PULPS

Authors: Claire Maulit, Rodger Beatson, Heather Trajano, Gloria Noki, Renz Po, Runxin Lai

Background

The objectives of this project are to: (1) understand the impact chemical treatments have on the development of fibre and fines' properties during LC refining, and (2) develop economically viable low energy processes that combine such treatments with LC refining to produce printing/writing, board and packaging grades.

Previous work by Chang et al. (2016) compared the effects of alkaline peroxide, chlorine dioxide, and ozone treatments with subsequent LC refining on TMP. Results showed that introducing oxidative agents reduces electrical energy consumption and improves pulp strength. Alkaline peroxide is hypothesized to generate acid groups on the surface of fibres and fines, increasing surface charge and causing surface fibre swelling. Swelling increases the bonded surface area and causes sheet densification. Chlorine dioxide and ozone oxidize lignin to produce carboxylic acids. A subsequent alkali soak forms sodium salt, which brings about softening and swelling of fibres and fines, leading to increase in tensile strength.

The current approach to optimize these technologies includes studying the kinetics of strength development during highly alkaline peroxide treatment (HAPT), and determining the contribution of fines to the property development of handsheets. The rate of increase in tensile strength during HAPT is assumed to be dependent on temperature, the concentration of hydroxide ion (pH) and concentration of hydrogen peroxide. To provide a basis for the kinetic studies, we have determined how these chemical concentrations change during HAPT. Furthermore, as strength development is linked to acid group generation, we have investigated the kinetics of acid group development in the fibre and fines.

Experimental

pH and Residual Hydrogen Peroxide During HAPT

The secondary refiner TMP used in the HAPT study was provided by Holmen Bråviken. Two batches of pulp were treated with 6% sodium hydroxide (NaOH) and 3% sodium silicate (Na_2SiO_3) for up to 120 minutes. The pulp consistency was 10% and the treatment conditions were varied as follows:

Pulp Batch	Hydrogen Peroxide (H_2O_2) Concentration	Temperature
1 – June 2022	2%	65°C, 75°C and 85°C
2 – November 2022	6%	65°C

The final pH and COD were measured using the filtrate collected after HAPT. Residual peroxide was measured using iodometric titration with 0.1 N sodium thiosulfate as the titrant. Weak acid content was determined using conductometric titration (June 2022 Newsletter).

Highly Alkaline Peroxide Treatment

The TMP was chelated with a 0.2% charge diethylene triamine pentaacetic acid (DTPA) at 4% consistency at 60°C in a water bath for 30 minutes. The pulp was then washed with deionized (DI) water with recirculation of filtrate to retain fines.

The chelated pulp was treated in a plastic bag at 75°C and a 20% consistency for 5 and 15 minutes with the following charges of chemicals based on oven dried (OD) pulp: 4% H_2O_2, 6% NaOH, 3% Na_2SiO_3. The pulp was mixed with the chemical solution by squeezing the bag. After treatment the pulp was washed as described above.

Kinetics of acid group generation in fibres and fines

The secondary refiner TMP used in the study of acid group generation in fibres and fines was provided by Alberta Newsprint Company. The HAPT protocol was as described above.

Separation of Fibers and Fines

20g OD pulp was hot disintegrated using standard procedures. DI water was added to achieve 0.5% consistency. The suspension was then placed in a 200 mesh "basket." 16L of DI water was run through to wash the fibres. Constant agitation was applied using a Sommerville Shive agitator to prevent cake formation. The fines passing through the mesh were dewatered by settling and syphoning before collection.

Determination of pulp properties

Handsheets were prepared according to TAPPI standard methods. Handsheet properties were determined according to TAPPI standards.

PROJECT 1.3

Results

Change in hydrogen peroxide concentration and pH during HAPT

Figure 1 shows that in the absence of pulp, the peroxide concentration drops rapidly during the first 30 minutes. The rate of peroxide loss increases with increase in both temperature and peroxide concentration. This is consistent with Guo et al. (2012), wherein the decomposition of H_2O_2 in NaOH solution is reported to be pseudo-second order with an activation energy of 110 kJ/mol.

At 75°C and 2% H_2O_2, the addition of pulp causes the percent residual H2O2 to drop more rapidly during the first 5 minutes of treatment time. After 5 minutes, the addition of pulp causes the consumption of 6.85 g H_2O_2 per 100 g pulp for 2% H_2O_2 at 75°C and 1.4 g H_2O_2 per 100 g for 6% H_2O_2 at 65°C. With an initial charge of 2% H_2O_2, the residual peroxide percentage with and without pulp are approximately equal after 60 minutes (Figure 2a). The faster drop in peroxide residual during the first 5 minutes can be attributed to peroxide being consumed by reaction with the pulp. The final pH as a function of treatment time at 75°C and 2% H_2O_2 is shown in Figure 2b. In this case the pH remains above 12 in both the presence and absence of pulp, which is consistent with loss of residual peroxide (Figure 2a).

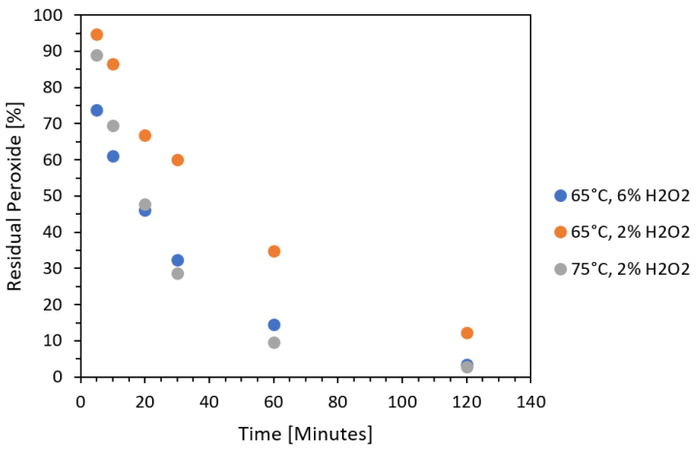

Figure 1. Percentage residual peroxide decreases over treatment time at varying temperatures and H_2O_2 concentrations.

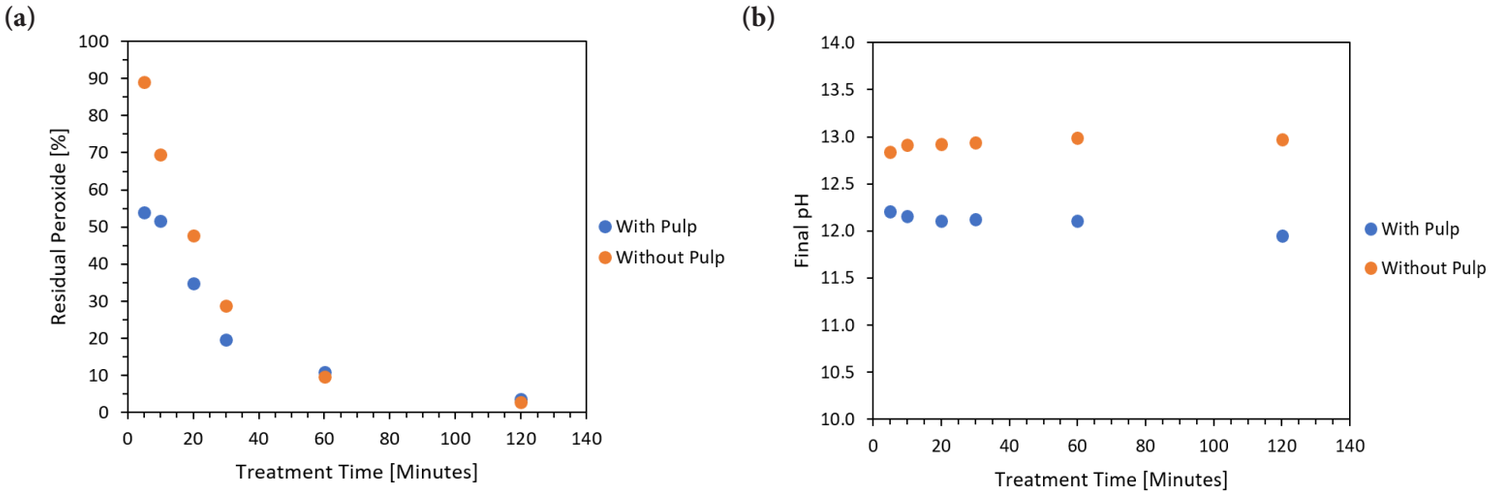

Figure 2. (a) Percentage residual peroxide of 2% H_2O_2 with and without pulp decreases over treatment time at 75°C; **(b)** Final pH with and without pulp as a function of treatment time at 2% $H_2O_2$and 75°C. Pulp received from Holmen Bråviken in June 2022.

PROJECT 1.3

When the initial peroxide charge was increased from 2% to 6%, the change in the percent residual peroxide during the first 5 minutes is smaller (Figure 3a). It is to be noted that at the higher initial charge of H_2O_2 and lower temperature, the percent residual at 120 minutes is much higher in the presence of pulp. When HAPT was conducted with 6% H_2O_2 at 65°C with pulp, there is an initial pH drop and then pH continues to fall. This decrease in pH was greater than was observed for HAPT with 2% H_2O_2 at 75°C with pulp. We hypothesize that the residual peroxide available after a higher initial charge caused slow generation of acid groups within the fibre and that these acid groups consume more alkali. The consumption of alkali by the newly formed acid groups contributes to the pH decrease, which in turn would lead to higher peroxide stability (Guo et al., 2012). Further investigation of the combined effects of acid group generation, H_2O_2 consumption, and pH is needed.

The increase in pH in the absence of pulp (Figure 3b) reflects the decrease in H_2O_2 in solution as H_2O_2 lowers pH through formation of the hydroperoxide anion.

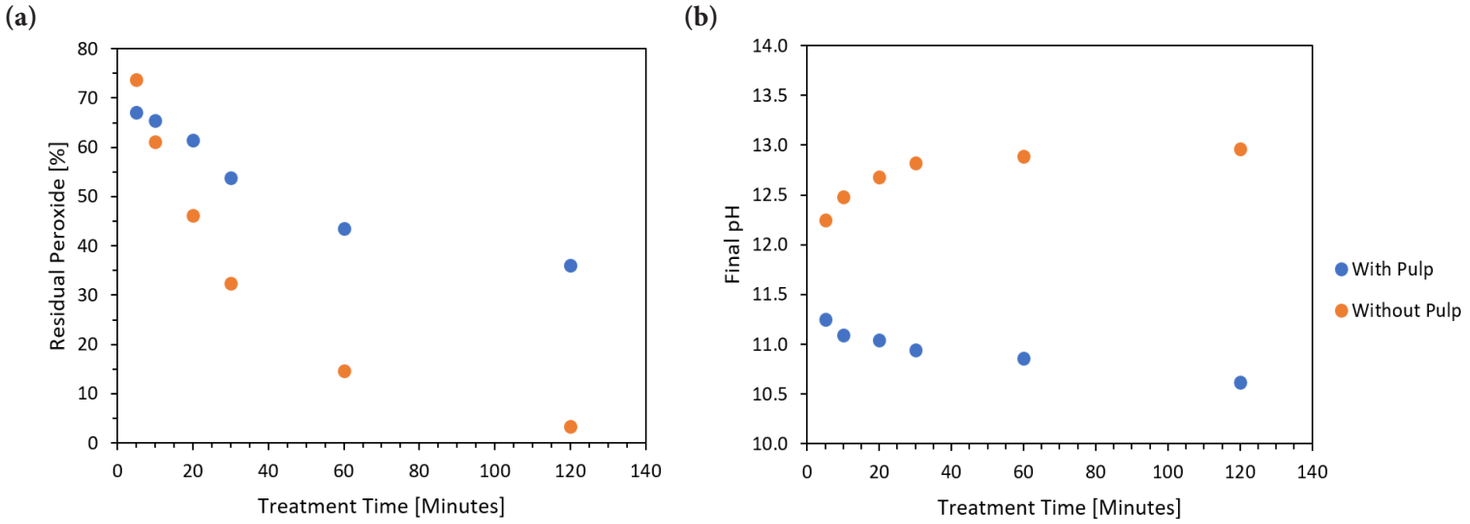

Figure 3. (a) Percentage residual peroxide of 6% H_2O_2 with and without pulp decreases over treatment time at 65°C; **(b)** Final pH with and without pulp as a function of treatment time at 6% H_2O_2 and 65°C. Pulp received from Holmen Bråviken in November 2022.

Changes in pulp properties during HAPT

The tensile strength of pulp increases rapidly during HAPT with gains of 10 to 13 N·m/g during the first 20 minutes (Figure 4) as predicted by the rapid consumption of peroxide by the pulp (2022 November Newsletter). Beyond 30 minutes, strength gains are minimal and the tensile strength plateaus at approximately 46 N·m/g. A charge of 2% H_2O_2 is sufficient to develop strength using HAPT. If strength is the only goal then additional H_2O_2 is unnecessary. This confirms our prior analysis (Chang et al., 2016). It is apparent that the H_2O_2 consumption during the initial stages of HAPT at both charges drives the strength gains.

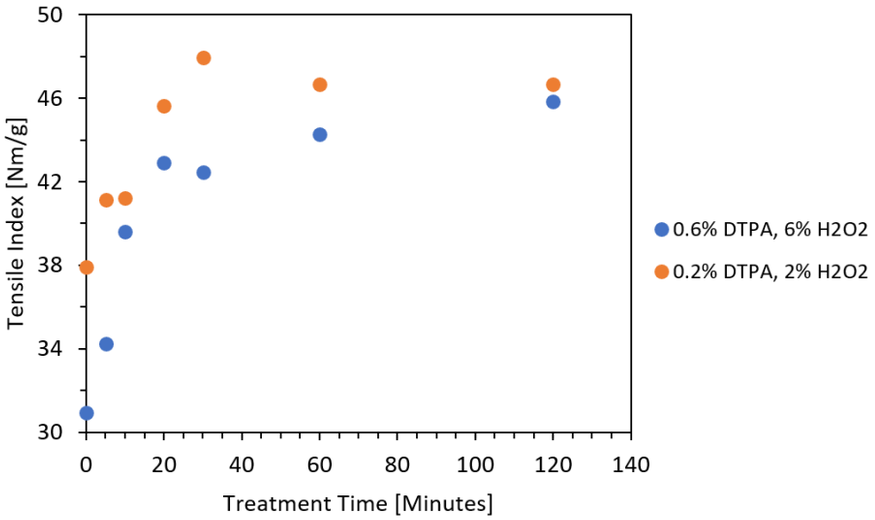

Figure 4. Tensile strength develops within the first 5 minutes of treatment for 0.6% DTPA, 6% H_2O_2 and 0.2% DTPA, 2% H_2O_2 at 65°C. Pulp for 2% H_2O_2 and 6% H_2O_2 received from Holmen Bråviken in June and November 2022, respectively.

PROJECT 1.3

However, if good brightness and strength development are simultaneously desired, then a high charge of H_2O_2 is beneficial (Figure 5). Both bulk and scattering coefficient decrease with increasing tensile strength, consistent with increased bonded area (Figures 6 and 7).

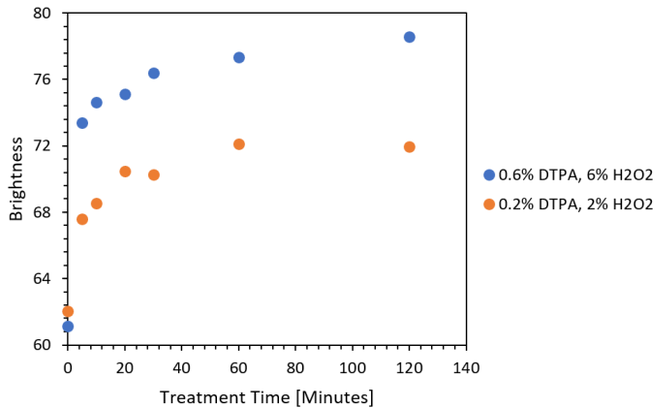

Figure 5. Brightness increases over treatment time for 0.6% DTPA, 6% H_2O_2 and 0.2% DTPA, 2% H_2O_2 at 65°C. Pulp for 2% H_2O_2 and 6% H_2O_2 received from Holmen Bråviken in June and November 2022, respectively.

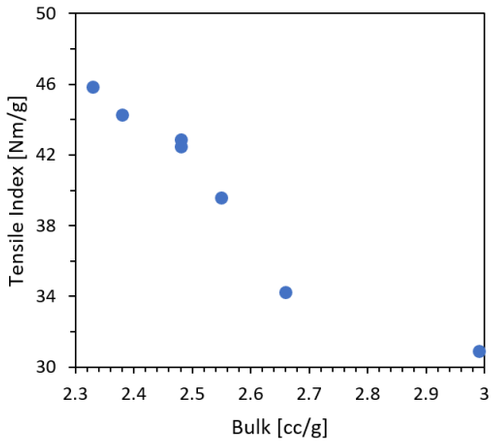

Figure 6. Tensile decreases with bulk for 6% H_2O_2 at 65°C. Pulp received from Holmen Bråviken in November 2022.

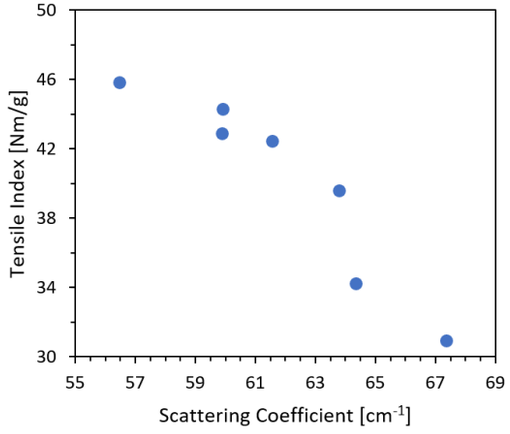

Figure 7. Tensile decreases with light scattering coefficient for 6% H_2O_2 at 65°C. Pulp received from Holmen Bråviken in November 2022.

Previously, we hypothesized that the carboxylic acid groups generated by the reaction of peroxide with the pulp and ionised in the presence of alkali lead to swelling of surfaces of the fibres and fines, which increases bonding. As shown in Figure 8, a correlation between acid group content and tensile index was observed. At equal acid group content, the pulp treated with 2% H_2O_2 had greater tensile strength than the pulp treated with 6% H_2O_2. We hypothesize that the spatial distribution of acid groups between fines, external fibre surfaces and internal fibre surfaces may be responsible for this difference.

In the November 2021 Newsletter, we demonstrated that HAPT treated fines play a large role in strength development. As shown in Figure 9, during HAPT treatment acid group generation occurs much more rapidly in the fines, reaching over 300 mmol/kg pulp within 5 minutes of treatment, than in the fibres. After 5 minutes, further acid generation primarily occurs in the fibres. The rate of acid group generation seems to be diffusion limited. Due to their small size and large surface area, fines provide easy access for the H_2O_2. In contrast, for reaction to occur in the fibre, chemicals must diffuse into the fibre wall. Rapid reaction of the alkaline peroxide with the fines leading to formation of acid groups occurs on the same time scale as tensile strength development.

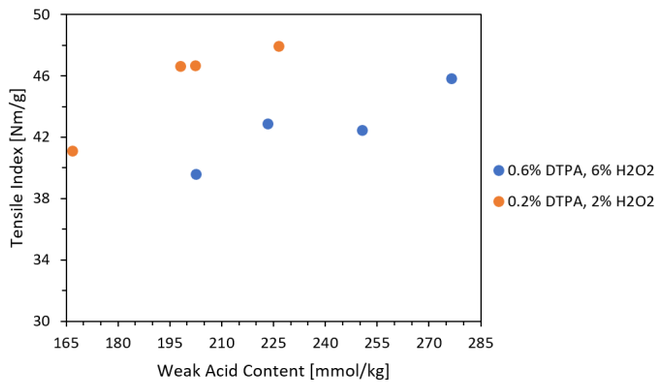

Figure 8. Tensile strength increases with weak acid content for 0.6% at 65°C. Pulp for 2% H_2O_2 and 6% H_2O_2 received from Holmen Bråviken in June and November 2022, respectively.

PROJECT 1.3

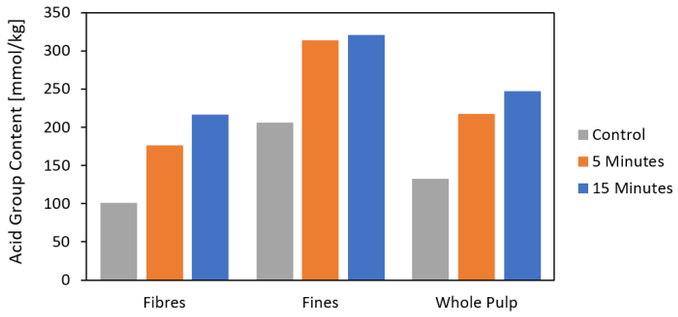

Figure 9. Acid group content of fibres, fines and whole pulp. Pulp received from Alberta Newsprint.

Conclusions

During the initial stages of the reaction, alkaline peroxide reacts rapidly and primarily with fines. This occurs on the same time scale as tensile strength development. Therefore, we hypothesize that reaction with fines promotes rapid development of tensile strength. There is a correlation between the development of tensile strength and acid group generation. Treatment with 2% H_2O_2 appeared to be as effective as 6% H_2O_2 in the development of pulp strength. Decreasing tensile strength with increasing bulk and scattering coefficient indicate that strength development is a result of increased bonded area.

Future Research

Future work will focus on verifying the hypotheses presented including (1) acid groups are first preferentially generated on fines and external fibre surfaces then within fibre structures due to mass transfer, and (2) acid groups on fines and external fibre surfaces are responsible for development of tensile strength.

References

1. Beatson, R., Trajano, H., Mitra, S., K., and Maulit, C. (2021, November). ERMP November 2021 Newsletter. Energy Reduction in Mechanical Pulping. https://ermp.sites.olt.ubc.ca/files/2022/06/ERMP_Nov2021.pdf
2. Chang, X. F., Luukkonen, A., Olson, J., & Beatson, R. (2016). Pilot-scale investigation into the effects of alkaline peroxide pre-treatments on low-consistency refining of primary refined softwood TMP. Bioresources, 11(1), 2030-2042. https://doi.org/10.15376/biores.11.1.2030-2042
3. Cheng, X. F., Olson, J. A., & Beatson, R. P. (2011). A comparison between the effects of ozone and alkaline peroxide treatments on TMP properties and subsequent low consistency refining. Bioresources, 7(1), 99-111. https://doi.org/10.15376/biores.7.1.99-111
4. Dence, C., W., and Omori, S., (1996). Survey of hydrogen peroxide bleaching of mechanical and (chemi)mechanical pulp - factors affecting brightness. Pulp Bleaching: Principles and Practice: TAPPI 1996, pp. 457-489.
5. Engstrand, P., Sjogren, B., Olander, K., and Htun, M., (1991). The significance of carboxylic groups for the physical properties of mechanical pulp fibres. 6th International Symposium Wood Pulping Chemistry, pp. 75-79.
6. Guo, T. X., Zhao, Y., Ma, S. C., & Liu, S. T. (2012, December 13). Decomposition characteristics of hydrogen peroxide in sodium hydroxide solution. Advanced Materials Research, 610-613, 359-362. https://www.scientific.net/AMR.610-613.359
7. Maulit, C., Beatson, R., Trajano, H., Po, R., and Lai, R. (2022, November). ERMP November 2022 Newsletter. Energy Reduction in Mechanical Pulping.
8. Mitra, S., K., Maulit, C., Beatson, R., and Trajano, H. (2022, June). ERMP June 2022 Newsletter. Energy Reduction in Mechanical Pulping. https://ermp.sites.olt.ubc.ca/files/2023/01/ERMP_June2022.pdf
9. Moldenius, S., (1984). The Effects of Peroxide Bleaching on the Strength and Surface Properties of Mechanical Pulping. Journal of Pulp and Paper Science., vol. 10, pp. 172-177.
10. Qin, C., Zeng, H., Liu, B., Zhu, J., Wang, F., Wang, S., Liang, C., Huang, C., Ma, J., & Yao, S. (2022). Efficient removal of residual lignin from eucalyptus pulp via high-concentration chlorine dioxide treatment and its effect on the properties of residual solids. Bioresource Technology, 360, 127621-127621. https://doi.org/10.1016/j.biortech.2022.12762

PROJECT 2.1

LIGNIN RICH FINES: SIMPLE ROUTES TOWARDS CREATION OF HYDROPHOBIC AND HYDROPHILIC FILLER ADDITIVES

Authors: Adam Wu, Siwei Chen, and Scott Renneckar

Background

As illustrated in the previous report, this project focuses on utilizing the unique characteristics of fines obtained from softwood thermomechanical pulp (TMP) and perform modification to enhance either hydrophobic or hydrophilic properties to expand opportunities. The primary objective of sub-project 1 is to enhance the hydrophobicity of TMP fines through chemical modification. This modification aims to create biomass-based additives for PLA, specifically for 3D printing applications. The previous report demonstrated that treating TMP fines with dodecenyl succinic anhydride (DDSA) through esterification substantially increased their hydrophobicity. The current report builds upon this approach. Conversely, sub-project 2 aims to improve the hydrophilicity of TMP fines, which is crucial when utilizing them as strength additives in the paper manufacturing process. A similar chemical reaction, esterification, is employed in this sub-project, utilizing succinic anhydride (SA) to convert the hydroxyl groups of TMP fines into carboxylic acid groups, thereby enhancing their hydrophilicity.

Sub-project 1: Hydrophobic fines

Initially, surface modification through esterification using alkenyl succinic anhydride compounds, for example, DDSA and octenyl succinic anhydride (OSA), was considered as an efficient method to enhance the distribution of fines in organic non-polar solvents. Successful surface modification was confirmed using FTIR spectroscopy, which demonstrated the introduction of functional groups, long hydrocarbon chains either 8 or 12 carbon in chain length, on the surface of fines. The increased hydrophobicity of the modified fines was demonstrated through water contact angle measurements, attributed to the substitution of long aliphatic chains for the hydroxyl groups on the surface. However, this approach did not effectively avoid the formation of fine aggregates after the reaction. As an alternative, ball milling without chemical modification was employed to reduce the size of fines and achieve a uniform dispersion of ball milled (BmTMP) fines in PLA.

The effects of ball milling on the size of fines were investigated by optical microscopy and laser diffraction. The microscope images (Figure 1a, b) showed TMP fines were reduced to smaller pieces. Although some unbroken fine fibres remained, more fragments could be observed following ball milling. Laser diffraction quantified the impact of ball milling on the particle size distribution of the fines, suggesting the same trend (Figure 1c). During the measurement, both unmodified TMP fines and BmTMP fines exhibited multi-modal distributions in water, with larger sizes potentially caused by particle agglomeration (Laouchedi et al., 2017). After ball milling, fines demonstrated more particle size distributions below 10 µm and smaller agglomerate distributions above 100 µm. The volume mean diameter ($D_{4,3}$) decreased from 77.56 µm to 45.2 µm, which also confirmed a reduced average particle size of BmTMP fines (Han et al., 2021).

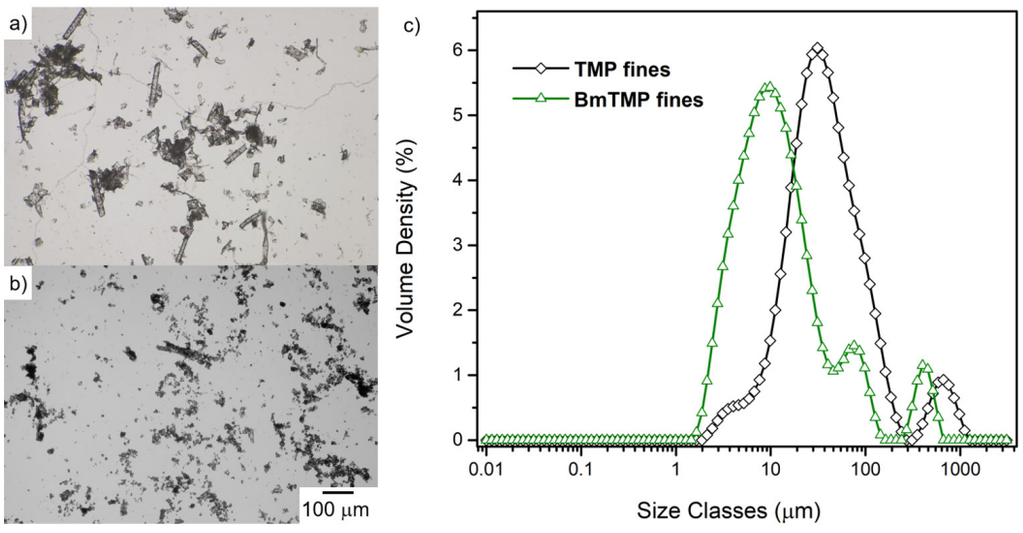

Figure 1. Microscope images of fines a) TMP fines, b) BmTMP fines, c) Particle size distribution of fines

PROJECT 2.1

To understand the performance of the PLA composites, including commercially available and lab-synthesized variants, the mechanical properties of various PLA composites were evaluated. The two commercial composites were Ingeo PLA 3D850 and Bamboo wood PLA with approximately 10% bamboo fillers with a different formulation. The rest of fine-based PLA composites comprised Ingeo PLA with TMP fines (as-is) and BmTMP fines at 10% and 20% concentrations, as well as Ingeo PLA containing 10% OSA and DDSA- modified fines. As expected, the tensile modulus, stiffness, increased with the addition of fillers and higher fibre contents, resulting in a greater tensile modulus (Figure 2a). This is because wood fillers are rigid and stiff materials in comparison to most thermoplastics (Lendvai et al., 2023). Pure PLA demonstrated the highest tensile strength at 62 MPa (Figure 2b), with an elongation at break of around 20% (Figure 2c). The commercial sample of BambooPLA showed unusual elongation properties in comparison. The reason for Bamboo PLA's higher strain at break could be attributed to the effect of the plasticizer added during the commercial manufacturing process. While the introduction of fine fillers slightly reduced tensile strength and significantly elongation at break, the weak interfacial adhesion between fines and PLA was identified as a possible cause for the brittle behaviour. As confirmed below by scanning electron microscope (SEM), fines disrupted the continuity of the PLA matrix and acted as stress concentration points as suggested by previous work (Moradi and Yeganeh, 2020). Interestingly, the tensile strength decreased more when increasing the TMP fines from 10% to 20% compared to BmTMP fines at the same loading. This suggests that ball milling aided fines in mitigating their negative impact on the PLA matrix. A slight increase in elongation at break was observed when raising the content of BmTMP fines from 10% to 20%, although further analyses are required to explain this phenomenon.

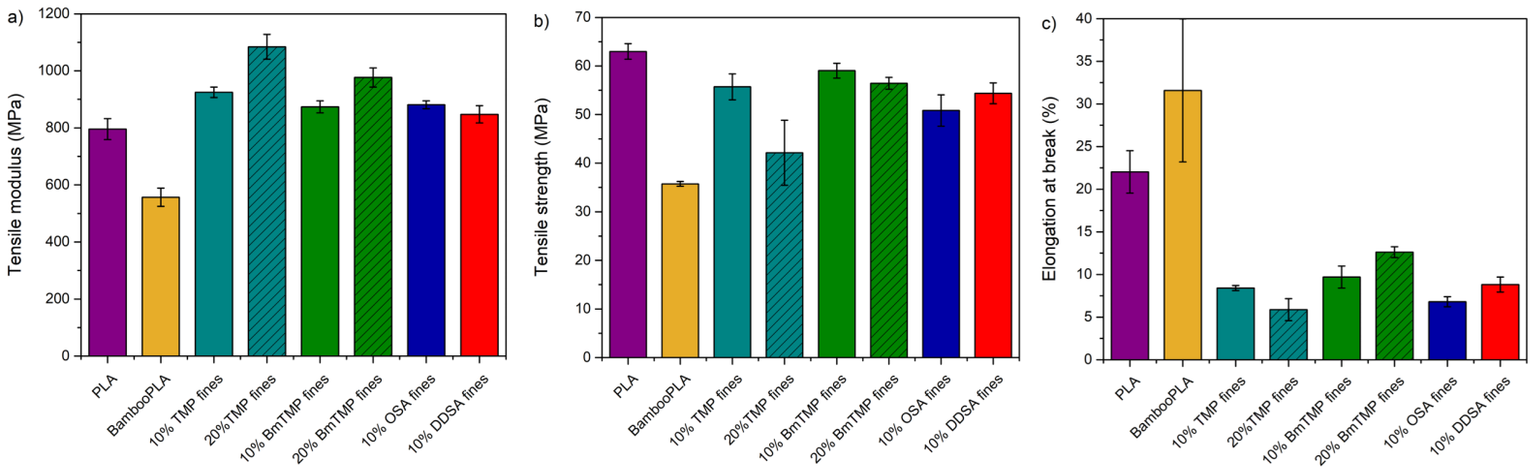

Figure 2. a) Tensile modulus, b) Tensile strength, c) Elongation at break of PLA, Bamboo PLA and PLA/fine Composites

Subsequently, the tensile fracture surface of the composites was evaluated by SEM to study the morphology of the PLA and PLA/fine composites. Figure 3 shows the representative images of the pure PLA, PLA-10% TMP fines, and PLA-10% BmTMP fines, PLA-10% OSA fines and PLA-10% DDSA fines respectively. The fracture surface of PLA appeared smooth and flat, with observed drawing fibrils suggesting the influence of a higher strain rate (Todo and Takayam, 2011). In contrast, the addition of fines resulted in a significant increase in surface roughness. Apparent fine aggregates were visibly present at the PLA-10% TMP fine interface, surrounded by large and deep cracks. These cracks indicate a brittle structure caused by stress concentrators arising from poor bonding between the more hydrophilic surface of the fines and the hydrophobic surface of PLA (Tao et al., 2017). Upon closer examination, various-sized cavities with encapsulated fines were also observed in other composites. This phenomenon suggests that the interfacial strength between the fines and PLA is weaker than the cohesive strength of the fines themselves (Pilla et al., 2009). Consequently, when subjected to external tensile forces, the fibres protrude outward, resulting in irregular holes on the fracture surface.

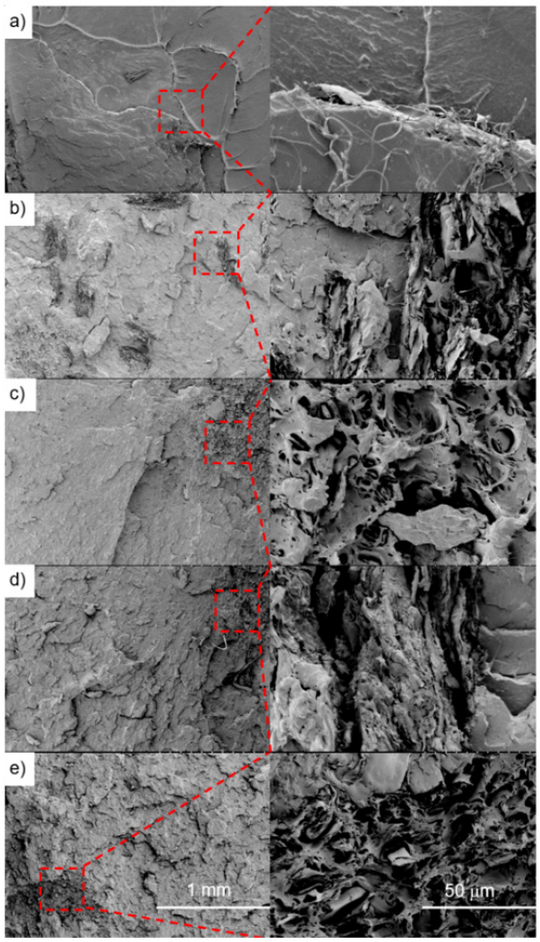

Figure 3. SEM images of a) pure PLA, PLA composites with b) 10% TMP fines, c) 10% BmTMP fines, d) 10% OSA fines, e) 10% DDSA fines.

To further elucidate the impact of fines addition to the stiffness of PLA, Differential Scanning Calorimetry (DSC) was employed to study the crystallization behaviour of both PLA and PLA/fine composites as crystallinity has been considered highly relevant to the stiffness of polymeric materials. The obtained thermograms are presented in Figure 4, while Table 1 provides the corresponding numerical values during the first heating cycle. The thermograms revealed that all tested composites exhibited peaks related to glass transition effect, cold crystallization, recrystallization, and melting. The incorporation of fines had a minimal impact on the glass transition temperature (Tg) values of PLA. With the introduction of chemically modified fines, the Tg experienced a slight decrease, implying that PLA was softened by modified fines on a molecular scale (Fico et al., 2022). Additionally, the inclusion of these modified fines resulted in a reduction of the temperature of cold crystallization (Tcc) and an increase in the enthalpy of cold crystallization compared to neat PLA. This effect can be attributed to fines acting as nucleating agents, thereby promoting the initial cold crystallization of the PLA matrix (Kuciel et al., 2020). However, the degree of crystallinity (Xc) did not increase in the PLA composites. On the contrary, the presence of fines throughout the composites hindered crystallite growth and the mobility of long polymer chains, leading to a decrease in crystallinity (Fazita et al., 2015). Despite the lower crystallinity observed in PLA composites compared to virgin PLA, their tensile modulus exhibited an increase due to the presence of stiff wood fibres.

Table 1. Thermal Characteristics of the PLA and PLA/fines Composites.

	Tg (°C)	Tcc (°C)	Tm (°C)	ΔHcc (J/g)	ΔHm (J/g)	Xc (%)
PLA	67.66	95.58	177.83	10.95	52.19	44.01
10% TMP fines	68.83	93.46	177.31	16.15	48.92	38.86
10% BmTMP fines	68.67	95.05	177.83	11.67	47.79	42.83
10% OSA fines	64.39	90.73	173.38	38.82	55.37	19.63
10% DDSA fines	64.99	91.28	175.93	18.02	53.50	42.07

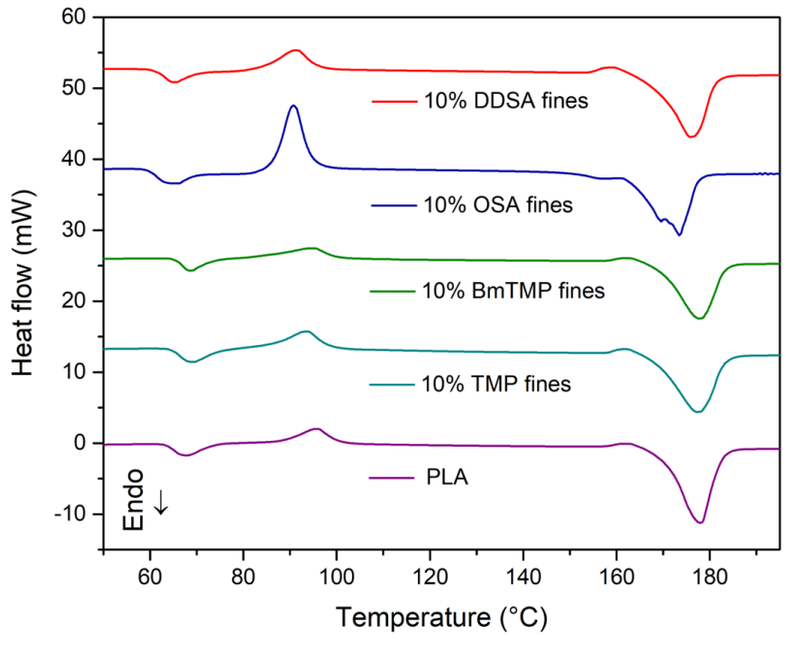

Figure 4. Melting curves of the PLA and PLA/fines composites (first heating cycle)

PROJECT 2.1

Sub-project 2: Hydrophilic fines

In continuation of the previous work led by Dr. Liyang Liu, we conducted a repetition of the modification process for mechanical pulp fines using succinic anhydride (SA) and imidazole to form N-succinylimidazole structure for rapid modification under mild conditions, following the method outlined by Beaumont et al., 2021. In addition to the purely chemical modification, we also explored an enzyme-mediated treatment approach by combining laccase and lytic polysaccharide monooxygenases (LPMO). Previous research by Chandra et al. has shown that laccase, when combined with gallic acid, can enhance the hydrophilicity of pulp. On the other hand, LPMO has been proven to oxidize the cellulose component of biomass by targeting the C1 and/or C4 carbon of the glucose unit (Song et al., 2018). However, our preliminary test using combined treatment of laccase, LPMO, and gallic acid did not result in a significant increase in the carboxylic acid content of the fines as compared to the SA treatment (Figure 5). This outcome is likely attributable to the high lignin content present in the fines (42% according to compositional analysis), which obstructs the access of LPMO to the cellulose component. Further work might be required to investigate the possible synergistic action between laccase and LPMO in order to overcome the recalcitrant nature of softwood mechanical fines to enzyme-mediated reactions.

Considering the superior effectiveness of chemical modification using succinic anhydride (SA) compared to enzyme treatments, we opted for this procedure in our subsequent work, which aimed to enhance the mechanical properties of hand-sheets derived from mechanical pulp. Alongside chemical modification, we also subjected the SA-treated fines to microfluidization, a commonly employed technique for producing cellulose nanofibrils. Despite the presence of lignin posing challenges to the nano-fibrillation of mechanical fines, the process resulted in a more uniform particle size distribution ranging from 50-70µm, as opposed to the previous range of 40-100 µm (Figure 6). As a starting point, fines undergoing these varying treatments were cast into sheets/films. The chemical and physicochemical modification of the fines led to a noticeable improvement in the mechanical properties of the films produced from various fines samples. Notably, the combined treatment of SA and microfluidization yielded a 48-fold increase in tensile strength and a remarkable 168-fold increase in Young's Modulus (Table 2). These findings clearly indicate that the modification process strengthened the hydrogen bonding between individual fines, suggesting that these modified fines would have a more significant impact on the mechanical properties of pulp when utilized as additives.

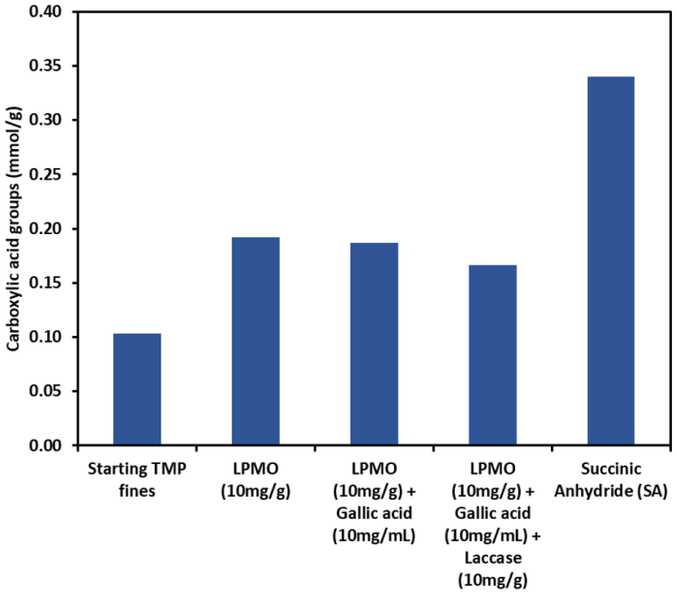

Figure 5. Carboxylic acid content of starting and modified TMP fines as measured by conductometric titration

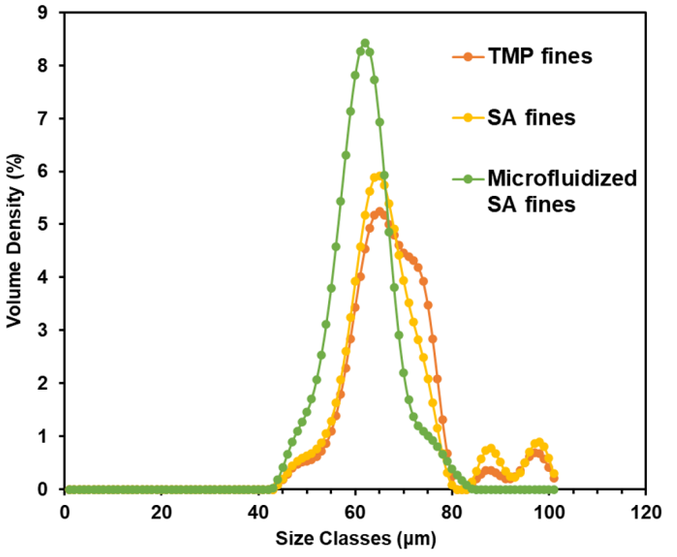

Figure 6. Particle size distribution of fines before and after chemical/ microfluidizer treatment

Table 2. Mechanical properties of films made from various fines samples

	Tensile stress at Maximum load (MPa)	Young's Modulus (GPa)
TMP fines	0.88	0.02
SA fines	16.75	1.12
Microfluidizer treated SA fines	43.24	3.38

After observing promising features in SA-modified TMP fines on their own, our next step was to investigate the potential enhancement of pulp mechanical properties by substituting 10 wt.% of regular TMP pulp (unbleached softwood mechanical pulp TMP provided by Holmen, Sweden) with the fines. However, as depicted in Figure 7, we found only minor improvement in tensile strength, while the tear and burst indices of the resulting hand sheets decreased after the addition of unmodified and modified fines. This decrease can be attributed to the high content of fines in the pulp, which likely hindered the beneficial effect of adding modified fines. It should be noted the original TMP contained a high content of fines as determined with a Fibre Quality Analyzer.

Additionally, cationic starch, a commonly used filler in the pulp and paper industry to enhance paper strength, was examined in conjunction with fines addition to regular TMP pulp (Sharma et al., 2020). We hypothesized that the positively charged cationic starch could interact with negatively charged SA-modified fines through electrostatic interactions. As expected, the inclusion of cationic starch (3 wt.% of pulp) improved the tensile strength of TMP supplemented with both TMP fines and SA fines. However, we were unable to test the effect of microfluidizer-treated SA fines due to equipment malfunction. After future repair, we anticipate a significant impact based on the current data described below.

Consequently, the addition of cationic starch, in conjunction with the various fine treatments further enhanced the tensile index of the resulting hand-sheets to around 15% (Figure 7a). Increases in burst index were observed when substituting TMP pulp with SA fines, including those treated with a microfluidizer (Figure 7b). The supplementation of cationic starch enhanced the beneficial effect of fines addition, even when adding unmodified TMP fines. However, in all scenarios, substituting TMP pulp with fines (with or without the supplementation of cationic starch) resulted in a decreased tear index of the resulting hand-sheet. Previous studies have suggested that fines-induced improvements in tear strength can reach their maximum level with very low fines content (Odabas et al., 2016). It is likely that the fines content in the original TMP pulp was already too high for the additional fines to provide significant benefits.

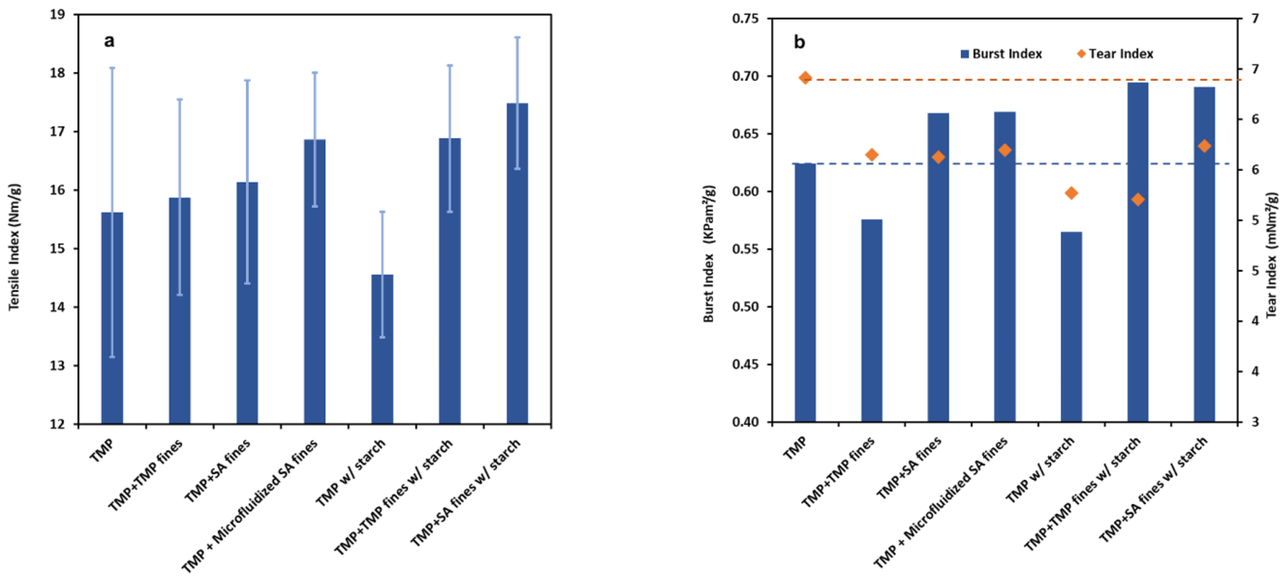

Figure 7. Tensile (a) Burst and Tear (b) indices of hand-sheets derived from TMP with and without the addition of various additives (fines and cationic starch)

PROJECT 2.1

Future Research

Sub-project 1: To examine the distribution of fines within the PLA matrix, the confocal microscope will be used to track the fillers, as it provides better contrast between the two materials compared to SEM. In terms of the DSC, further data and analysis from the cooling cycle, employing a lower cooling rate, as well as the second heating cycle, are also required. These experiments will allow for a direct comparison of the crystallization behaviour of the various materials while eliminating any previous thermal history established during the first heating cycle. As well, with minimal differences observed with chemical modification, we will add a commercial "coupling agent" to melt and process the fines along with the PLA. We plan on the creation of 3D printing filaments with the various fine modifications to create prototype 3-D printed materials.

Sub-project 2: Based on the obtained results, it is evident that our chemical and physicochemical modification of TMP fines holds potential as fillers for paper-making applications. However, the presence of a high fines content in the original TMP pulp appears to hinder this improvement. Consequently, future work will focus on assessing the impact of modified fines on mechanical pulp with a lower initial fines content. This can be achieved either by removing fines from the current TMP pulp using the Bauer-McNett fibers classifier and adding back in the modified fines into the system.

Acknowledgements

We would like to thank our undergraduate research assistant, Nicole Ting, for her invaluable contribution to the experimental sessions.

References

1. Beaumont, M., Tardy, B.L., Reyes, G., Koso, T. V., Schaubmayr, E., Jusner, P., King, A.W.T., Dagastine, R.R., Potthast, A., Rojas, O.J., Rosenau, T., 2021. Assembling Native Elementary Cellulose Nanofibrils via a Reversible and Regioselective Surface Functionalization. J. Am. Chem. Soc. 143, 17040–17046.
2. Chandra, R.P., Lehtonen, L.K., Ragauskas, A.J., 2004. Modification of High Lignin Content Kraft Pulps with Laccase to Improve Paper Strength Properties. 1. Laccase Treatment in the Presence of Gallic Acid. Biotechnol. Prog. 20, 255–261.
3. Fazita, M.R.N., Jayaraman, K., Bhattacharyya, D., Hossain, M.S., Haafiz, M.K.M., Abdul Khalil, H.P.S., 2015. Disposal options of bamboo fabric-reinforced poly(lactic) acid composites for sustainable packaging: Biodegradability and recyclability. Polymers (Basel). 7, 1476–1496.
4. Fico, D., Rizzo, D., De Carolis, V., Montagna, F., Palumbo, E., Corcione, C.E., 2022. Development and characterization of sustainable PLA/Olive wood waste composites for rehabilitation applications using Fused Filament Fabrication (FFF). J. Build. Eng. 56, 104673.
5. Han, J., Fitzpatrick, J., Cronin, K., Maidannyk, V., Miao, S., 2021. Particle size, powder properties and the breakage behaviour of infant milk formula. J. Food Eng. 292, 110367.
6. Kuciel, S., Mazur, K., Hebda, M., 2020. The Influence of Wood and Basalt Fibres on Mechanical, Thermal and Hydrothermal Properties of PLA Composites. J. Polym. Environ. 28, 1204–1215.
7. Laouchedi, D., Bezzazi, B., Aribi, C., 2017. Elaboration and characterization of composite material based on epoxy resin and clay fillers. J. Appl. Res. Technol. 15, 190–204.
8. Lendvai, L., Omastova, M., Patnaik, A., Dogossy, G., Singh, T., 2023. Valorization of Waste Wood Flour and Rice Husk in Poly(Lactic Acid)-Based Hybrid Biocomposites. J. Polym. Environ. 31, 541–551.
9. Moradi, S., Yeganeh, J.K., 2020. Highly toughened poly(lactic acid) (PLA) prepared through melt blending with ethylene-co-vinyl acetate (EVA) copolymer and simultaneous addition of hydrophilic silica nanoparticles and block copolymer compatibilizer. Polym. Test. 91, 106735.
10. Odabas, N., Henniges, U., Potthast, A., Rosenau, T., 2016. Cellulosic fines: Properties and effects. Prog. Mater. Sci. 83, 574–594.
11. Pilla, S., Gong, S., O'Neill, E., Yang, L., Rowell, R.M., 2009. Polylactide-Recycled Wood Fiber Composites. ournal Appl. Polym. Sci. 111, 37–47.
12. Sharma, M., Aguado, R., Murtinho, D., Valente, A.J.M., Mendes De Sousa, A.P., Ferreira, P.J.T., 2020. A review on cationic starch and nanocellulose as paper coating components. Int. J. Biol. Macromol. 162, 578–598.
13. Song, B., Li, B., Wang, X., Shen, W., Park, S., Collings, C., Feng, A., Smith, S.J., Walton, J.D., Ding, S.Y., 2018. Real-time imaging reveals that lytic polysaccharide monooxygenase promotes cellulase activity by increasing cellulose accessibility. Biotechnol. Biofuels 11, 1–11.
14. Tao, Y., Wang, H., Li, Z., Li, P., Shi, S.Q., 2017. Development and application ofwood flour-filled polylactic acid composite filament for 3d printing. Materials (Basel). 10, 1–6. https://doi.org/10.3390/ma10040339
15. Todo, M., Takayam, T., 2011. Fracture Mechanisms of Biodegradable PLA and PLA/PCL Blends. Biomater. - Phys. Chem.

PROJECT 2.2

FROM TREES TO TREATMENT: FUNCTIONALIZING TMP EXTRACTIVES

Authors: Cameron Zheng, Juliana Lima de Freitas, Laurel Schafer, Heather Trajano

Background

Extractives such as terpenes are used as natural medicines.[1] The ability to modify their structures could create more potent therapeutics. Terpenes contain double bonds or olefinic bonds, this provides opportunity for functionalization via hydroaminoalkylation using the catalysts developed by the Schafer group. Hydroaminoalkylation is a reaction which adds a C—H bond adjacent to a nitrogen of an amine across a double bond.[2] Amination of β-pinene and limonene was previously demonstrated with our tantalum-catalyst using N-methylaniline (NMA) (Fig. 1). We will use this catalyst to create aminated terpenoids and aminated extractives. In this report, we describe the quantification and attempted optimization of turpentine (provided by Holmen Pulp) for hydroaminoalkylation.

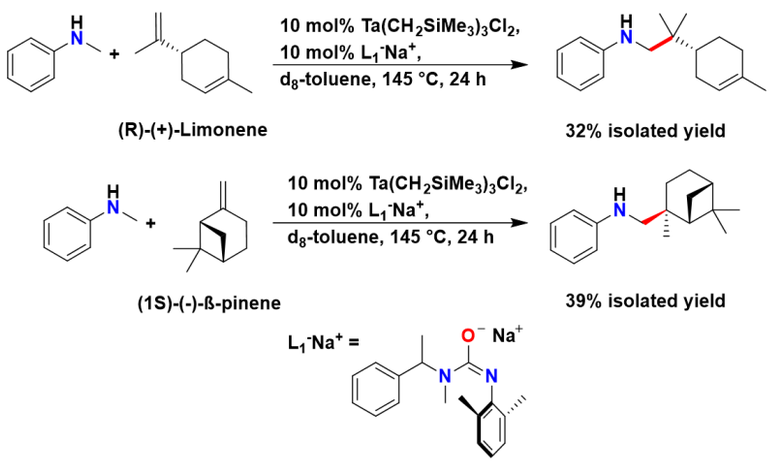

Figure 1. Reaction scheme for β-pinene and limonene amination by hydroaminoalkylation.[3]

Previously we concluded that the presence of linoleic acid and other fatty acids was the cause of undesirable odorous compounds in pulp. Unsaturated fatty acids, such as linoleic acid, contain double bonds and a carboxylic acid group. The double bonds are a candidate for hydroaminoalkylation but carboxylic acids are incompatible with our catalyst. In November 2022, we reported that a decarbonylative dehydration reaction removes the carboxylic acid to produce a compatible, reactive olefin. The olefin contains three double bonds and the terminal bond was aminated. In this newsletter, we report on efforts to aminate the previously untransformed double bonds.

Quantification and catalytic transformation of turpentine

Quantification of turpentine proceeded by dissolving 1 mmol of turpentine oil in 0.8 mL d_8-toluene followed by the addition of 0.33 mmol of 1,3,5-trimethoxybenzene as internal standard. Monoterpene content was quantified using $^1H\{^{13}C\}$ (quantitative) NMR spectroscopy where relaxation delay (d_1) was set to 100 seconds.

1:1 amine:reactive terpene experiment proceeded with 0.35 mmol of N-methylaniline (amine) and 1 mmol turpentine in 10 mol% of $Ta(CH_2SiMe_3)_3Cl_2$ and sodium ureate ligand (**L_1-Na^+**) dissolved in 1 mL toluene in a 2 dram vial. The vial was sealed and allowed to heat at 145 °C for 24 hours. After reaction completion, the reaction mixture was subjected to vacuum overnight then re-dissolved in 0.8 mL d_8-toluene and 0.05 mmol of 1,3,5-trimethoxybenzene was added. The solution was transferred to an NMR tube for quantitative NMR.

1 mmol amine for turpentine amination reaction proceeded with 1 mmol of each N-methylaniline and turpentine with same reaction set up and quantification as **1:1 amine:reactive terpene experiment.** Isolation of product molecules **1** and **2** (**Fig. 2B**) proceeded via filtration through silica gel with 9:1 hexanes:ethyl acetate as eluent.

Results

We had previously reported the amination of turpentine and antimicrobial screening using the aminated turpentine mixture by disk-diffusion assay. As turpentine is a mixture of monoterpenes and other essential oils, we hypothesized that the hydroaminoalkylation reaction efficiency could be further improved relative to the amount of amine used if we quantified the reactive terpenes, β-pinene and limonene (**Fig. 2**). Turpentine was determined to contain 26 mol% β-pinene and 9 mol% limonene, and 57 mol% α-pinene, which is non-reactive.

PROJECT 2.2

Results (cont.)

Quantification of turpentine composition also enabled us to calculate the NMR yield of 1 and 2 (Fig. 2A). NMR yields are measured in-situ, without isolation of products **1** and **2**, Isolated yield is measured after purification of **1** and **2**; the use of silica gel chromatography to complete the notoriously difficult isolation of amines results in some product loss. Isolated yield is thus always lower than NMR yield. Interestingly, the yield of **1** was comparable that of our previous work using purified β-pinene meaning that our catalyst is effective at selective amination within a complex terpene mixture.[3] Though the yield of 2 was higher than previously reported, this is likely due to the higher concentration of amine present in solution for the turpentine reaction. Furthermore, an isolated yield of 1 and 2 of 28% was obtained; products 1 and 2 were present as an inseparable mixture by silica gel chromatography with a 2:1 ratio.

As our total reactive monoterpene content of turpentine was 0.35 mmol, we attempted to lower the amine amount to create a 1:1 amine:reactive monoterpene ratio (**Fig. 2B**). Unfortunately, this resulted in lower NMR yields than the initial trial.

Increasing amination in decarbonylated dehydrated linoleic acid (Triene)

Previously, we removed the carboxylic acid functionality from linoleic acid (purchased from Combi-blocks) to produce a molecule containing 3 olefinic bonds, which we named triene. Catalytic upgrading of triene proceeded with 0.6 mmol of N-methylaniline and 0.2 mmol of triene in 5 mol% of $Ta(CH_2SiMe_3)_3Cl_2$ and sodium ureate ligand (L_1-Na^+ or L_2-Na^+) dissolved in 0.8 mL d_8-toluene in a 1 dram vial with 0.33 equivalents of 1,3,5-trimethoxybenzene added as internal standard. An ^1H Nuclear Magnetic Resonance (NMR) spectrum was taken of the solution before and after reaction at 130 °C or 140 °C to determine amination reaction progress.

Results

We hypothesized that a polyamine could be produced from triene if the amount of amine in the reaction mixture was increased to match the number of olefinic bonds. Polyamines are valuable in material applications because they can be used as hardeners in polyepoxides to alter mechanical, chemical, and heat resistance

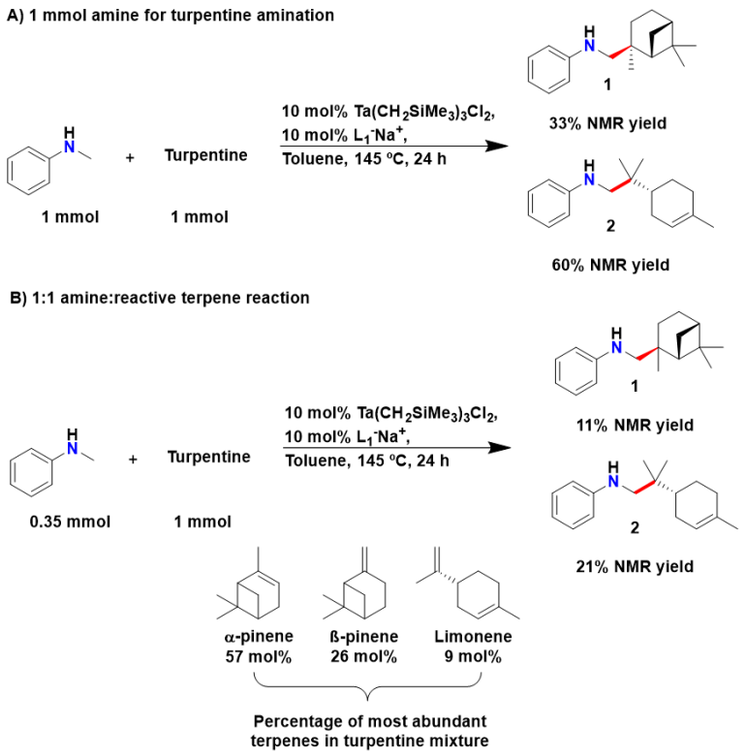

Figure 2. Quantification of turpentine and attempt at optimization of turpentine amination reaction relative to 26 mol% β-pinene and 9 mol% limonene in turpentine.

properties.[4] The equivalent of N-methylaniline was increased to a 3:1 ratio relative to triene (**Fig. 3A**). Unfortunately, only terminal olefin bond functionalization was observed.

Inspired by our group's work in the amination of existing olefin-containing polymers, we were motivated to apply a related catalyst which employs a different ligand for the transformation of internal olefinic bonds in triene (**Fig. 3B**).[5] The presence of a less sterically bulky ligand **L_2-Na^+** could facilitate internal olefinic bond. To our delight, we observed some of di-aminated product 4, though mono-aminated product 3 remained the major product. We believe that additional reaction optimization can be pursued by increasing catalyst loading or increasing reaction time and temperature to increase the yield of 4.

PROJECT 2.2

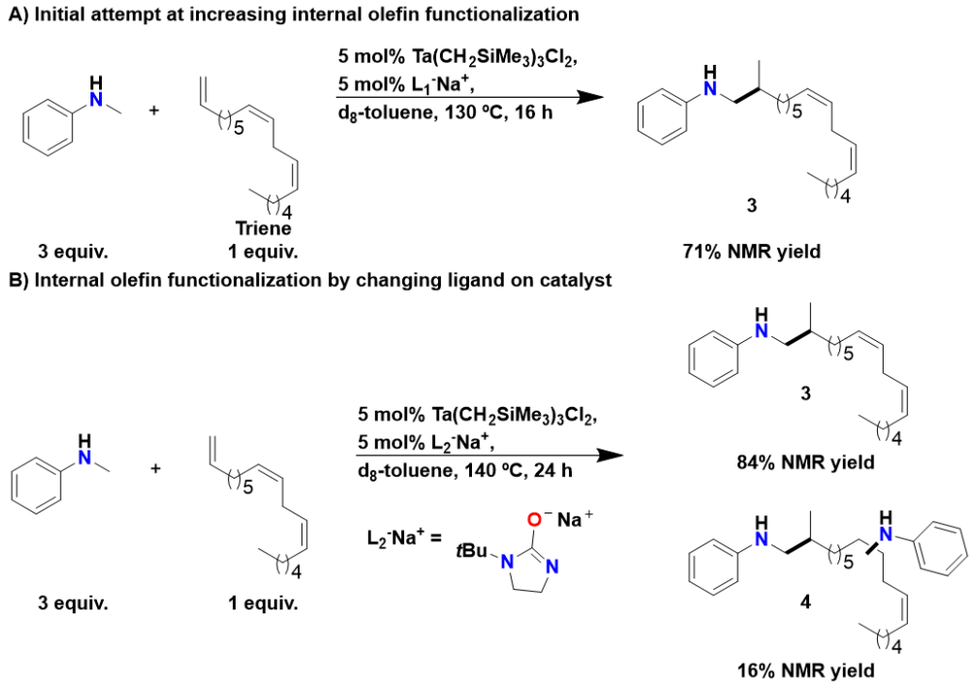

Figure 3. Functionalization of triene and efforts towards functionalizing internal olefins.

Future Research

The next steps of the project will focus on the recovery of fatty acids from the pulp mill environment. Recovered fatty acids will be transformed to olefin products and then subjected to amination.

Machine learning tools will be applied to correlate input data such as pH, temperature, solids, and COD to predict the amount and distribution of fatty acids in process water and/or wastewater. By adopting machine learning models, instead of relying solely on lab tests, we hope to lower costs and return results more rapidly. We will use this model to identify the points in the process and conditions that favour the presence of long-chain fatty acids, such as linoleic acids.

A second model will be developed to determine the most suitable liquid-liquid extraction technique and conditions to recover long-chain fatty acids. Lab tests will be used to verify model performance.

References

1. Cox-Georgian, D.; Ramadoss, N.; Dona, C.; Basu, C. Med. Plants From Farm to Pharm. 2019, 333–359.
2. DiPucchio, R. C.; Rosca, S.-C.; Schafer, L. L. J. Am. Chem. Soc. 2022, 144, 11459–11481.
3. DiPucchio, R. C.; Rosca, S.; Athavan, G.; Schafer, L. L. ChemCatChem 2019, 11, 3871–3876.
4. Froidevaux, V.; Negrell, C.; Caillol, S.; Pascault, J. P.; Boutevin, B. Chem. Rev. 2016, 116, 14181–14224.
5. Scott, S. S.; Roşca, S. C.; Gilmour, D. J.; Brant, P.; Schafer, L. L. ACS Macro Lett. 2021, 10, 1266–1272.

PROJECT 2.3

MFC PRODUCTION, CHARACTERIZATION, AND PROPERTIES OF MECHANICAL PULPS

Authors: Mariana Frias de Albuquerque, James Olson, Boris Stoeber, Heather Trajano

Background

This study addresses the low-energy production of microfibrillated cellulose (MFC) from mechanical pulp fines for various paper applications. In a previous phase of this project, we investigated the production of MFC using short fibres obtained from bleached chemi-thermo-mechanical pulp (BCTMP). The pulp was fractionated using different screens and then refined at the UBC Pulp and Paper Centre pilot plant. The refined short fibres were subsequently combined with long fibres, and paper handsheets were created for mechanical testing. The findings from this phase were published earlier this year (Seifert et al., 2023).

Building upon the initial investigation, we proceeded with fractionating BCTMP fibres using a 0.8 mm-hole screen. In 2022, we analyzed the refined short fibres as a function of refining energy levels, focusing on their rheological properties. The level of refinement was correlated with the storage modulus, which indicates the elasticity of fibre suspensions. Additionally, we developed protocols for enzymatic hydrolysis and characterization of fibrillation. The extent of fibrillation was determined by measuring the fibril perimeter using L&W+ tester (Canfor Pulp Innovation Centre) and linearly correlating it with the number of PFI revolutions.

Since the last ERMP Steering Committee meeting, we have evaluated the influence of pH and temperature during cellulase hydrolysis on the morphology of post-refining short fibres in the PFI mill, as well as the inter-fibre interaction through sedimentation tests. Rheological analysis and the effects of enzymatic incubation conditions have been documented in two manuscripts that are currently undergoing internal review. Brief summaries of the most recent results are provided in this document.

Results

The process parameters for enzymatic hydrolysis of short fibres with endoglucanase (EN) or a mixture of endo- and exoglucanase (EN+EX) prior to PFI refining are shown in Table 1. See below.

Table 1 Experimental matrix to assess the effect of incubation pH and temperature on fibre morphology.

Pulp Consistency (%)	Incubation Temperature (°C)	Incubation pH	Incubation Time (h)	Enzyme Dosage (wt. OD%)	Enzyme Type	PFI Revolutions
3.5	60 80	5 8	2	1.0*	Control (no enzyme) EN EN+EX	10,000

* In the case of the mixture of EN+EX, exoglucanase is an auxiliary enzyme. It is dosed as 10 wt.% of endoglucanases.

PROJECT 2.3

Results (cont.)

Fibre morphology

Figure 1 presents fibril perimeter (FP) values for fibres after incubation, both before and after PFI refining. FP is substantially influenced by incubation pH, temperature, and enzymatic hydrolysis conditions, and it generally increases significantly with refining.

For the control group, the highest post-refining FP value (28.3%) is obtained after incubation at pH 8 and 80°C, while the lowest (26.3%) occurs after incubation at pH 5 and 60°C. Incubation at pH 8 promotes higher fibrillation during refining compared to pH 5. We hypothesize that this is due to the deprotonation of carboxyl groups on the fibre surface causing the fibre surface to become more negatively charged thus increasing inter-fibre repulsion (Choi et al., 2016; Zhang et al., 1994). This, in turn, allows for better fibre dispersion and greater flexibility during the refining process, facilitating fibrillation. Such increased flexibility could enable fibres to withstand greater tensile strength. It is possible that alkaline incubation of short fibres can enhance the development of paper products with high bulk and tensile strength.

Fibres treated with EN exhibit a decrease in FP in comparison to the corresponding control group at every incubation condition. According to Orłowski et al. (2015), there is a negligible extent of enzyme penetration into the cell wall, and as a result, fibre modification is concentrated on the surface of the fibres. Due to higher accessibility, loose fibrils in amorphous areas are the first targets of endoglucanases. Thus, instead of forming new fibrils by peeling fibres, EN promotes the cleavage of the fibrils from the surface.

According to earlier kinetics essays provided by ABEnzymes, when incubated at pH 5, cellulase EN activity peaks at 60°C and significantly decreases when the temperature is raised to 80°C. Similarly, temperatures between 60°C and 65°C at pH 5 result in maximum EX activity. In fact, the pre-refining FP is slightly higher at 80°C suggesting reduced cleavage of fibrils, but the decrease in FP at 80°C compared to 60°C does not vary significantly with incubation conditions for fibres treated with EN, which suggests that enzyme kinetics are not the mechanism sole responsible for fibre morphology modification. Table 2 reports coarseness values for the post-refining samples. Samples treated with EN present lower coarseness when incubated at 60°C, which aligns with the hypothesis of fibril detachment from the fibre surface.

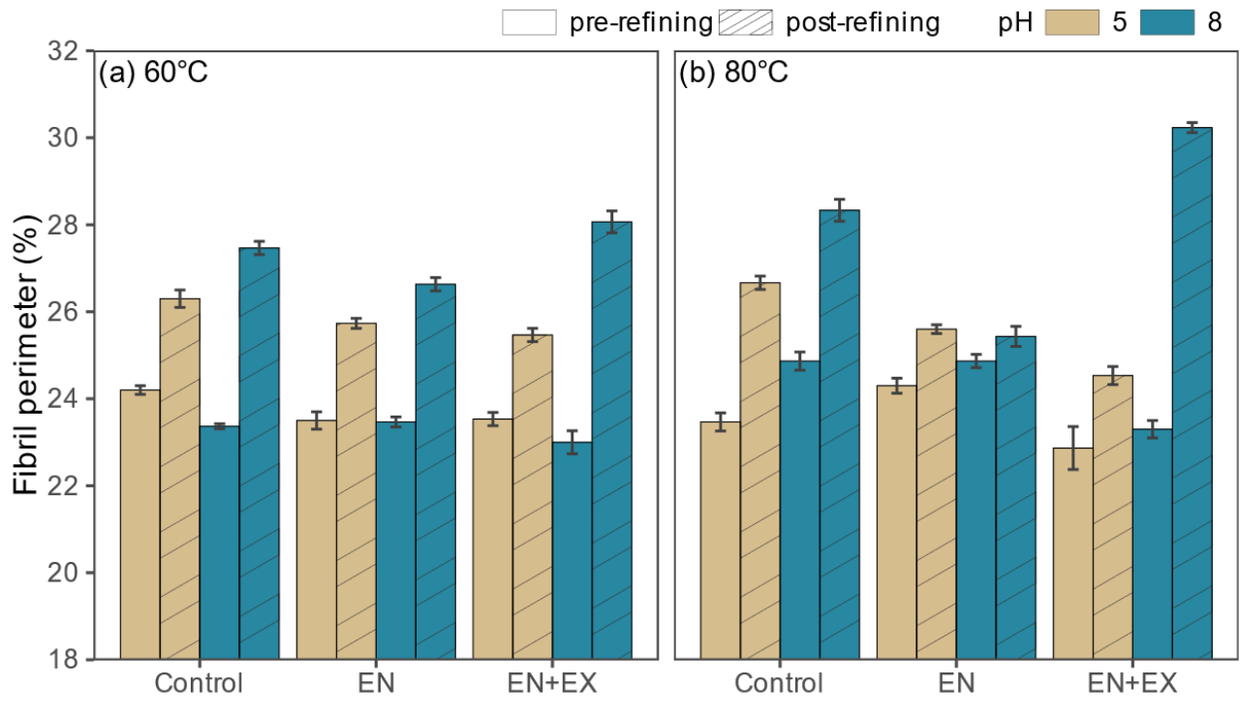

Figure 1. Average length weighted fibril perimeter of short fibres after enzyme hydrolysis at different pH and temperatures, pre- and post-refining in the PFI mill. Control samples were incubated at hydrolysis conditions, in the absence of enzymes, prior to refining.

PROJECT 2.3

Table 2 Coarseness values for BCTMP short fibres after incubation at different conditions and PFI refining.

Sample	pH	Temperature (ºC)	Coarseness (mg/100m)
Control	5	60	6.00 ± 0.02
		80	5.46 ± 0.02
	8	60	5.39 ± 0.04
		80	5.30 ± 0.01
EN	5	60	5.02 ± 0.03
		80	5.50 ± 0.02
	8	60	5.17 ± 0.04
		80	6.17 ± 0.03
EN+EX	5	60	4.73 ± 0.01
		80	5.60 ± 0.02
	8	60	4.43 ± 0.01
		80	4.21 ± 0.03

Finally, for fibres treated with EN+EX, fibrillation changes to a large extent with incubation pH. For pH 5, addition of 0.1% exoglucanase only slightly reduces FP for at both temperatures. However, for pH 8, divergent behaviour is observable. At 60°C and 80°C, refining of fibres hydrolyzed with EN+EX causes FP to increase by 22% and 30%, respectively. At 60°C, FP after refining (28.1%) is approximately equal to the control group incubated at pH 8. Fibres hydrolyzed with EN+EX at pH 8 and 80°C have the largest FP value post-refining among all investigated samples. Furthermore, these fibres present lower coarseness, or higher flexibility, suggesting that enzymatic hydrolysis at pH 8 and 80°C improves the reinforcement properties of the short fibres.

Interfibre interactions

Fibre settling is commonly associated with pulp drainage, filtration, and the formation of paper products. All fibres were washed and re-suspended in ultra-pure water (pH 7.2) for sedimentation tests. Figure 2 (i) shows the relative settling height for fibres incubated or enzymatically hydrolyzed and then refined. It has been reported that higher settling height indicates greater structural strength of the fibre network (Li et al., 2018). Thus, comparing the normalized final heights for each sample can provide insight into the influence of incubation conditions with or without enzymatic hydrolysis on the mechanical properties and formation of paper handsheets.

Enzymatic treatment at pH 5 and 60°C does not yield significant alterations in the final sedimentation height compared to the control group. At 80°C, fibres treated with EN display a slightly greater height than the control group. Conversely, those treated with EN+EX exhibit the lowest height among all the tested samples. Furthermore, there is a significant impact of incubation pH on sedimentation. Fibres incubated at pH 8 exhibit a greater settling height than those incubated at pH 5, regardless of temperature. In addition, the enzymatic treatment at pH 8 results in an increase in sedimentation height in comparison to control groups. While the EN+EX treatment at 60°C does not lead to a substantial increase in the settling height, at 80°C, the same treatment exhibits the highest settling height among all the evaluated samples.

Differences in fibre sedimentation can result from different morphologies. As previously discussed, incubation at higher pH leads to an increase in surface charge and the formation of a more open fibre network due to inter-fibre repulsion. Therefore, fibre morphology is not the sole factor determining settling height. This was assessed by thoroughly washing the refined samples and then resuspending them in distilled water followed by measurement of the water conductivity. Sample conductivity linearly correlates to relative sedimentation height, as shown in Fig. 2 (ii). This suggests that the increase in the conductivity of suspensions leads to an elevation in the sedimentation height. Sedimentation tests and suspension conductivity were also determined for short fibres refined at the UBC PPC Pilot Plant; these data are included in Fig. 2 (ii). Interestingly, the linear relation between settling height and conductivity is maintained even for fibres submitted to different refining mechanisms. Measuring suspension conductivity may be a rapid and facile technique to evaluate short fibre quality.

PROJECT 2.3

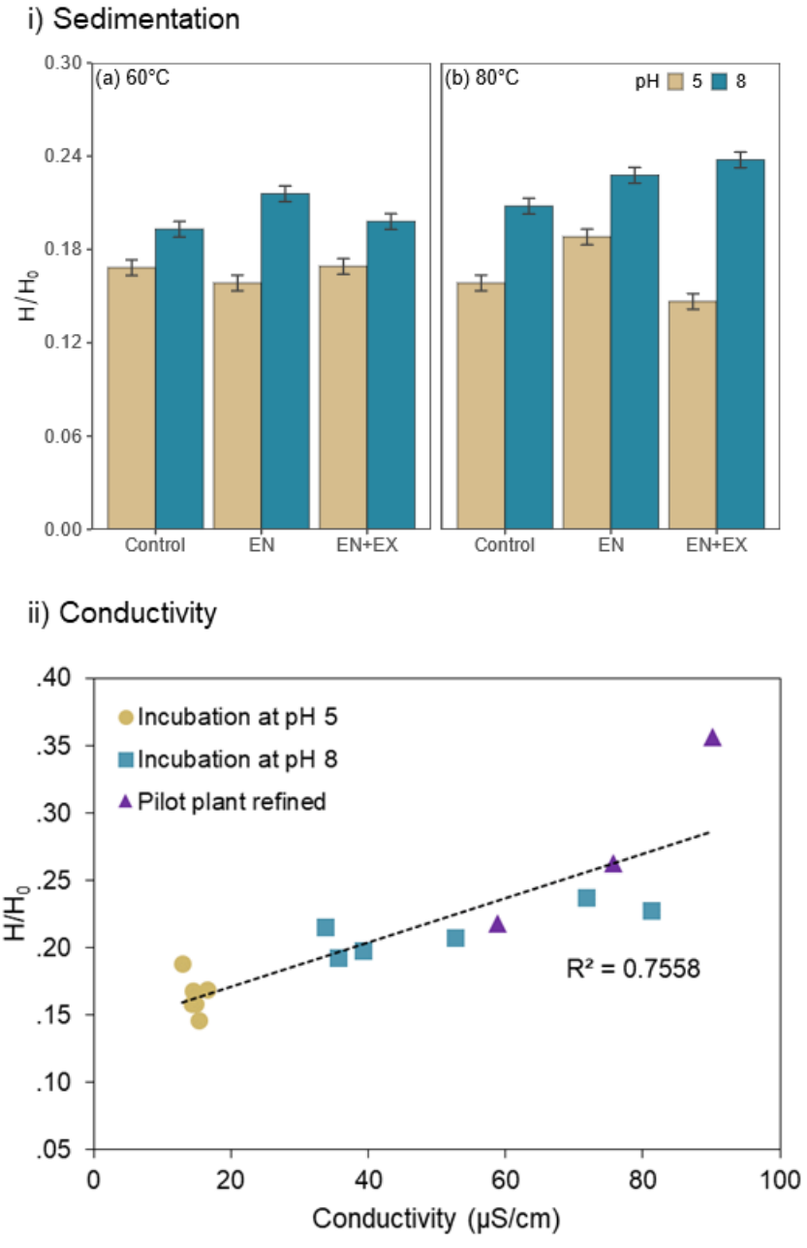

Figure 2 Relative settling height (H/H0) of short fibres after enzyme hydrolysis incubation at different pH and temperatures post-refining at the PFI mill (i); and the correlation between fibre conductivity and relative settling height (ii).

Future Research

We will continue with investigations regarding incubation conditions for enzymatic hydrolysis. We will analyze the effect of varying enzyme dosage, in addition to the ratio between endo- and exoglucanase. The goal is to find an enzyme dosage and combination that facilitates fibrillation but is financially viable for the industry.

In addition, we will perform enzymatic hydrolysis on a standard substrate under different incubation conditions to characterize enzyme kinetics independent of complex pulp composition and morphology.

Finally, paper handsheets will be produced to compare their tensile and bulk properties to sedimentation tests.

References

1. Choi, K.-H., Kim, A. R., & Cho, B.-U. (2016). Effects of Alkali Swelling and Beating Treatments on Properties of Kraft Pulp Fibres. BioResources, 11(2), 2.
2. Li, W., Yang, Y., Sha, J., Zhou, J., Qin, C., & Wang, S. (2018). The influence of mechanical refining treatments on the rheosedimentation properties of bleached softwood pulp suspensions. Cellulose, 25(6), 3609–3618.
3. Orłowski, A., Róg, T., Paavilainen, S., Manna, M., Heiskanen, I., Backfolk, K., Timonen, J., & Vattulainen, I. (2015). How endoglucanase enzymes act on cellulose nanofibrils: Role of amorphous regions revealed by atomistic simulations. Cellulose, 22(5), 2911–2925.
4. Seifert, R., Gharehkhani, S., Vargas Figueroa, D., Mercuur, J., & Olson, J. (2023). Engineering the paper production by combined fibre fractionation and reinforcement with microfibrillated cellulose. Cellulose, 30(5), 3201–3217.
5. Zhang, Y., Sjögren, B., Engstrand, P., & Htun, M. (1994). Determination of charged groups in mechanical pulp fibres and their influence on pulp properties. Journal of Wood Chemistry and Technology, 14(1), 83–102

PROJECT 3.1

CREATING BULKY FIBRES

Authors: Elisa Ferreira, Jason Sugiharto, Anderson Veiga, Emily Cranston, Mark Martinez

Background

In this project, our motivation is to overcome the paradigm "bulk versus tensile strength" in pulp refining using applied surface chemistry. A one-pot chemical modification is being designed to enhance bulk and mechanical properties of chemi-thermomechanical pulp (CTMP). We propose the use of hydroxypropyl methylcellulose (HPMC) as a binder that adsorbs irreversibly onto the cellulose surface. This chemical modification can be applied just after the pulping step as well as to the paper itself. HPMC is a low cost, renewable and FDA-approved water-soluble additive derived from cellulose. Favourable interactions between methylcelluloses and cellulose have previously been applied by our group to stabilize bio-based emulsions, gels and latexes (Hu et al., 2015; Kedzior et al., 2017). The hypothesis is that fibre-fibre bonds can be reinforced by HPMC through polymer entanglements and intermolecular forces. Besides mechanical performance, the adsorption of surface active HPMC on the fibre cell-wall is expected to reduce the interfacial tension inside the lumen, which could potentially prevent the fibre from collapsing due to capillary forces during drying.

Results

BCTMP handsheets were prepared with and without pressing. Two ways of incorporating HPMC were tested: (1) pre-treatment by adding HPMC into the pulp slurry, prior papermaking; (2) post-treatment by spraying HPMC solution onto paper handsheets to tailor tensile index and bulk. Our results show that both tensile index and bulk were greatly affected by pressing (Fig. 1). This mechanical process increased the density of the fibre network, which improved the tensile strength for all tested conditions.

For the pressed handsheets, post-treatment with HPMC improved both bulk and tensile index for all HPMC loads tested, without significant differences for HPMC loads between 0.5 and 1.5 wt% in water (20 to 60%, based on fibre mass). HPMC pre-treatment enhanced bulk and tensile index, indicating that the additive can be incorporated to add value to BCTMP pulp. Interestingly, bulk can be enhanced by simply rewetting paper, but with reduced tensile strength (white bars, Fig. 1) which we believe is specific to mechanical pulps. Morphological analysis by X-ray micro-computed tomography (μCT) showed fibres with open lumens in paper handsheets prepared without pressing and with HPMC pre-treatment and post-treatment (Fig. 2, see right).

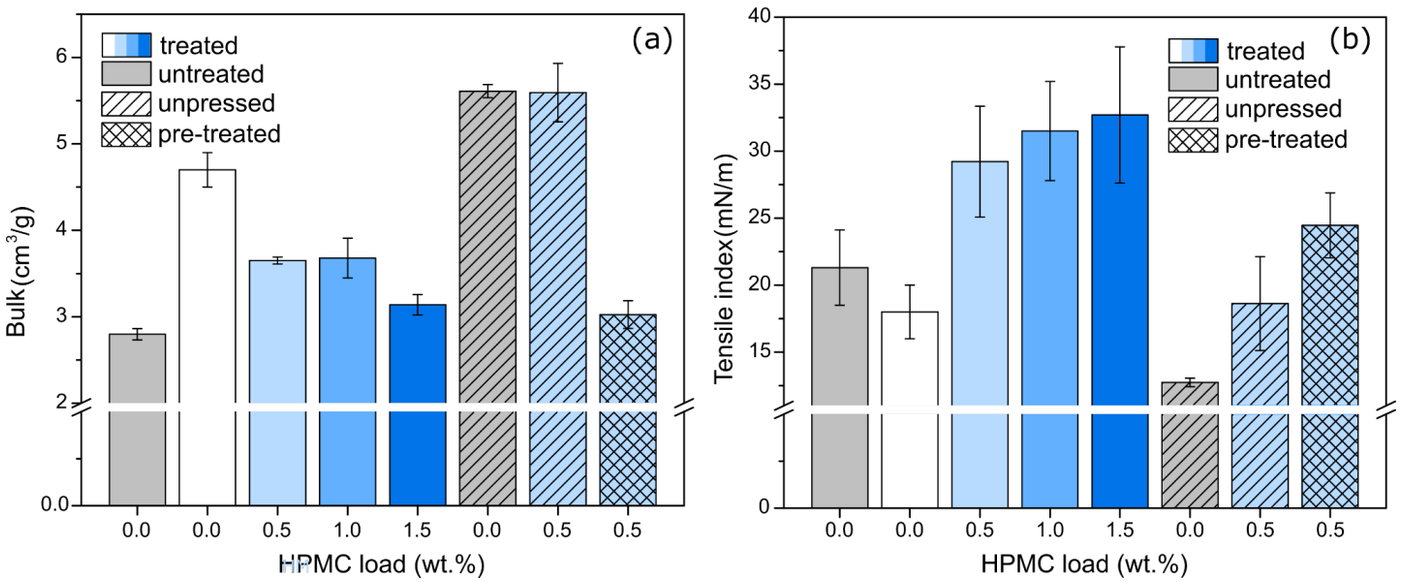

Figure 1. (a) Bulk and (b) tensile index of paper handsheets untreated, post-treated with HPMC (0 to 1.5%), unpressed, or pre-treated with HPMC. Highest bulk values were achieved for unpressed samples and the tensile index was enhanced by HPMC under all tested conditions

PROJECT 3.1

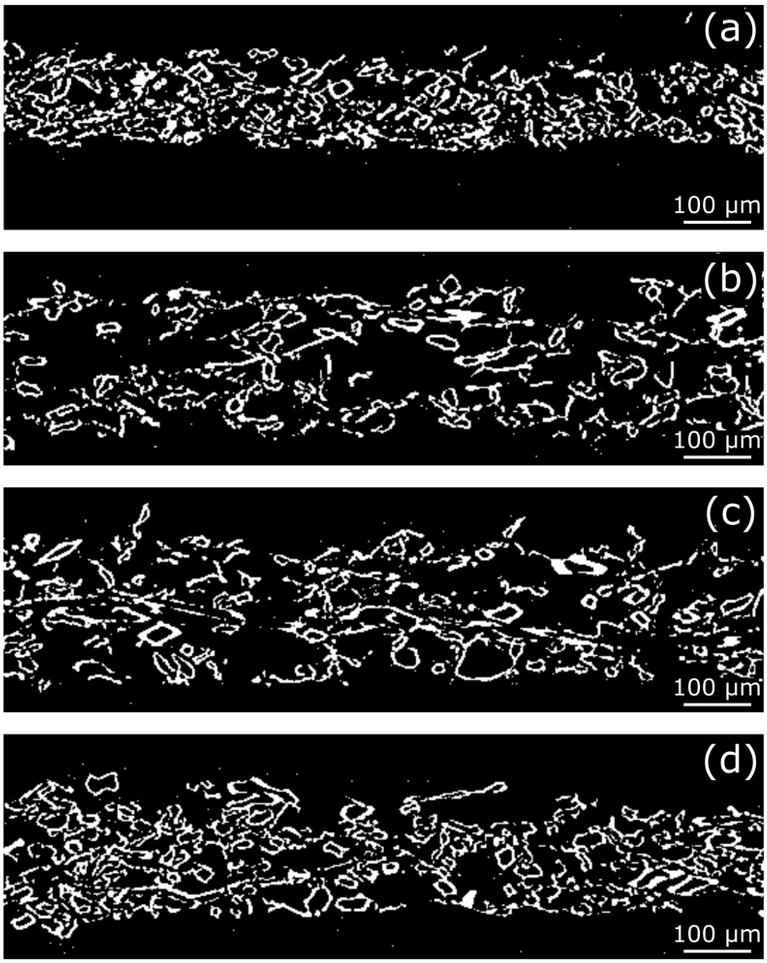

Figure 2. Reconstructed µCT images of paper handsheets: (a) untreated; (b) unpressed; (c) pre-treated with HPMC 0.5%; (d) post-treated (sprayed on handsheet) with HPMC 0.5%.

References

1. Hu, Z.; Patten, T.; Pelton, R.; Cranston, E. D. Synergistic Stabilization of Emulsions and Emulsion Gels with Water-Soluble Polymers and Cellulose Nanocrystals. ACS Sustain. Chem. Eng. 2015, 3 (5), 1023–1031.
2. Kedzior, S. A.; Dubé, M. A.; Cranston, E. D. Cellulose Nanocrystals and Methyl Cellulose as Costabilizers for Nanocomposite Latexes with Double Morphology. ACS Sustain. Chem. Eng. 2017, 5 (11), 10509–10517.

Results (cont.)

The pre-treatment with HPMC altered fibre properties, as revealed by fibre quality analysis (FQA, Table 1). The polymer adsorption increased the length and width of the fibres. The reduction in kink number and curl index with HPMC indicated that this additive favours fibres to unfold in water, which may promote better dispersion for paper formation. This is a novel approach that can be integrated in the paper making process, without requiring any chemical refining and additional drying step. Moreover, the low surface tension of HPMC should reduce the energy required in drying steps.

Future Research

In the next steps, data analysis using K-means clustering image will be performed to extract quantitative parameters from µCT data. Handsheets with HPMC pre and post-treatments will be evaluated in terms of thickness, pore size and distance between fibres. Our goal is to develop an approach to express the presence of open lumens in the modified samples. In future research, we will also evaluate the combination of HPMC, other surface active agents, and chemical cross-linkers to create bulky fibres with high tensile index.

Table 1. Fibre properties of pristine (control) BCTMP and BCTMP pre-treated with HPMC 0.5 wt%, as determined by FQA.

Sample	*Length (mm)*	*Width (µm)*	*Kinks per mm*	*Curl index*
Control	*1.32 ± 0.01*	*30.65 ± 0.05*	*0.405 ± 0.005*	*0.063 ± 0.002*
Pre-treated	*1.42 ± 0.01*	*31.65 ± 0.05*	*0.325 ± 0.005*	*0.052 ± 0.001*

PROJECT 3.2

ADVANCED CHARACTERIZATION – COMPUTED TOMOGRAPHY

Authors: Aurélien Sibellas, Sam Brown, Lewis Mason, James Drummond, André Phillion, Elisa Ferreira, Anderson de Veiga, Emily Cranston, Mark Martinez

Background

This project supports several other projects in this consortium through specific in-situ experimental protocols and advanced quantitative 3D microscopy. In the previous reporting periods, we reported on the development of imaging protocols for wood chips and CTMP hand-sheets, and, on image-processing algorithms to quantify the images. In this reporting period we have had two major activities:

a) We continued to develop our image quantification algorithms and have explored methodologies to enhance contrast using (i) tracers in conjunction with immersion oils and advanced denoising, and (ii) exploring machine learning to identify individual fibre species.

b) We continued to develop protocols to characterize the behavior of CTMP hand-sheets. In particular we made significant progress on our protocols to both understand stretch in paper and understand better water absorption.

Results

In this reporting period, we examined the potential of adding a small amount of labelled fibres into a BCTMP sheet in order to trace motion during tensile testing. To do so, we prepared handsheets containing 1% iron nanoparticles (Figure 1a) and measured the mechanical response of the sheet in comparison to a standard handsheet. We found that the ultimate tensile strength remains somewhat unaffected by the presence of the tracer at these low levels of addition, allowing us to proceed to the visualization portion of the work. The visualization portion of the work primarily focussed on segmenting the labeled fibres from the unlabeled ones. Two approaches were adopted to segment the tracer fibres:

(a) In the first approach we physically-treated the sample with an immersion oil, to mask air and the unlabeled fibres from the labelled fibres, and then digitally-enhanced the image using denoising algorithms (Figure 1b). As shown, enhanced contrast between the phases was achieved. This methodology gave quite promising results.

(b) In parallel with this, we examined a machine-learning methodology to directly segment the iron tracers from the original reconstruction. This was achieved by using a unique convolutional neural network (CNN) architecture as well as a custom layer to help with classifications (see Figure 1c). One useful product of this work is that we developed a novel method of binarization (Figure 1d).

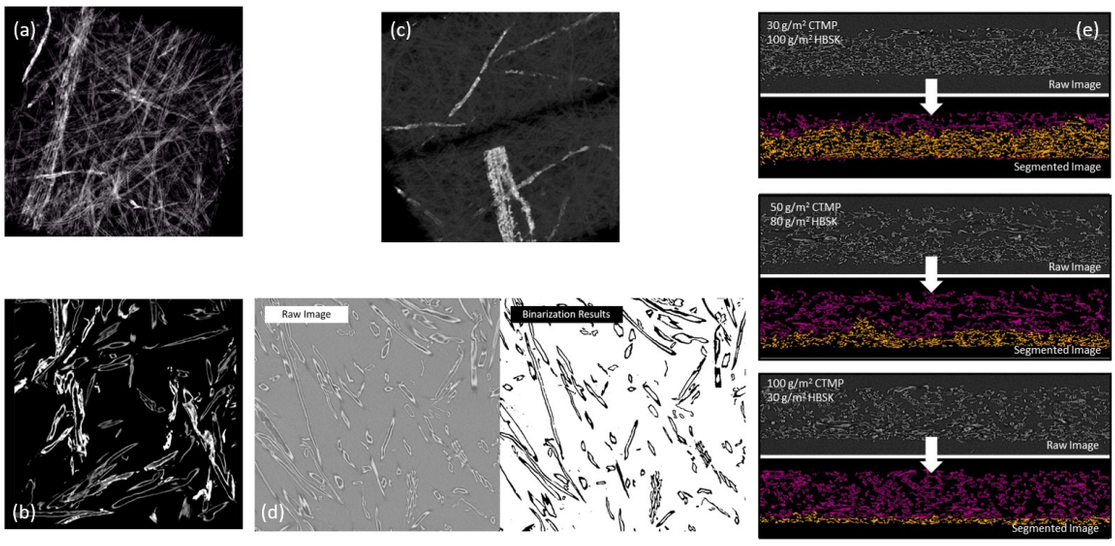

Figure 1. (a) BCTMP long fibres (length ~ 3.5 mm) containing 7% in volume of iron oxide NPs in relation to the total volume of pulp fibres were incorporated at a weight percentage of 1% (b) 3D rendering of iron labeled tracers using a combination of immersion oil and denoising. (c) Using a machine-learning approach to segment the iron labelled fibres in a BCTMP sample.(d) An improved thresholding methodology to binarize the tomographic images. (e) Using a machine learning approach to segment layered handsheets.

PROJECT 3.2

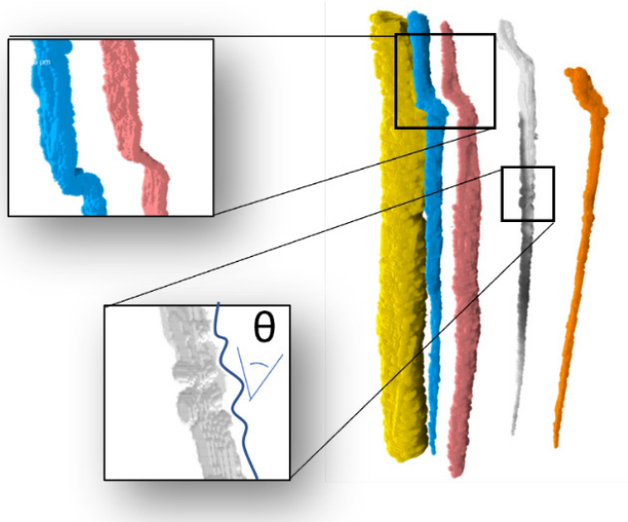

Figure 2. Isolated fibres from the 10th compression step (3% strain) showing buckling and microcompressions. All fibres pictured show buckling, yet microcompressions are only apparent in the white-coloured fibre.

In addition, we have started a collaborative project with VTT (Tuomas Turpeinen, Jyvskyla Finland) to develop computational tools that enable the identification of fibre type in sheets made from a mixture of fibre species. As shown in Figure 1e, three distinct composites of HBSK/CTMP are shown, formed through a layering process. In each case we were successful in identifying the layered region.

In the previous reporting period we presented new algorithms that characterized both paper samples and wood chips, and created a plug-and-play software package for image analysis (Sibellas, 2022). We also reported on an experimental study of aspen wood under compression and the potential to apply iron nanoparticles as tracers for mapping the liquid percolation in paper (Ferreira et al., 2023). In this reporting period, we continued our study of aspen wood under uniaxial compression via X-ray microtomography. In particular, we examined the mechanism of forming microcompressions in wood fibres as compared to buckling, as shown in Figure 2. Literature results have shown that paper products made using microcompressed fibres possess superior extensibility properties, whereas the occurrence of buckling within the mechanical pulping process negatively impacts tensile strength.

Using an in-situ compression device, an aspen wood sample was compressed 300 µm over 10 steps, 30 µm per step. A 3D tomogram was acquired at each step, with a 1.2 µm3 voxel size. Deformation of individual fibres was tracked from one step to the other using our in-house image analysis tools. This analysis revealed that fibres began to buckle slightly after only 2% compressive strain. Therefore, the identified critical strain limit of 2% may serve as an effective pre-treatment for wood chips in the Impressifiner.

Future Research

Further studies on water absorption are underway to continue the work from the previous update. Last period, we reported on the use of x-ray microtomography to study the imbibition of liquids into paper sheets by measuring the precipitation of iron tracers. Now, we plan to expand the study to include the use of several different imaging modalities to quantify the dynamics and locations of imbibition at different scales. To begin, we are using macro photography to measure and visualize the dynamics of the precursor and post-wetting fronts at the millimeter scale. These measurements will be verified on a smaller scale using swept-field laser confocal microscopy to measure the imbibition of fluorescent dyes. We will then continue x-ray microtomography studies, this time adding innovative approaches involving masking wood fibres using immersion oil, and deep learning-based tomographic reconstruction and segmentation. Through international collaborators, we also have access to a synchrotron light source and X-ray Nanotomography. Unlike our in-laboratory tomograph, the synchrotron light source can capture quickly evolving dynamics, which we will use to study the 4D behaviour of imbibition. Using the nanotomography, we hope to measure the 3D flow through inter- and intra-fibre pores during imbibition.

References

1. Sibellas, A., Litjens, J., Drummond, J., Phillion, A.B. & Martinez, D.M., “Visualization of monodisperse fibre assemblies during compression” Fundamental Research Society in Pulp and Paper Research, Cambridge (2022)

2. Ferreira, E. S., Drummond, J., Veiga, A. T. V., Sibellas, A., Brown, S., Cranston, E. D., Martinez, D. M. Mapping absorbency in cellulosic fibres with iron tracers. Carbohydrate Polymers (2023), 311, 120785.

ERMP PERSONNEL UPDATES

FAREWELLS

In recent times, the ERMP group has bid farewell to postdoctoral fellows: Dr. Aurelien Sibellas, Dr. Elisa Ferreira, Dr. Rasmita Sahoo and Dr. Samira Gharehkhani, and graduate student Claire Maulit. We wish them the best as they embark on new career paths and extend our appreciation for their significant contributions to the ERMP program throughout their time with us. In addition, we would like to acknowledge the efforts of our undergraduate students, Hamza Dastgir and Salman Dajani. They joined us at the end of 2022 and the beginning of 2023, respectively, providing invaluable support to our ongoing research and trials at the PPC Pilot plant. Their dedication and hard work in processing the data for Project 1.1 have been greatly appreciated.

NEW ARRIVALS

Additionally, we are thrilled to introduce the talented individuals who have recently joined the UBC Pulp and Paper Center. We encourage you to take a moment to familiarize yourselves with their backgrounds and read their introductory profiles below.

Postdoctoral fellows

Fariba Yeganeh

Dr. Fariba Yeganeh received her Ph.D. degree in Organic Chemistry in 2022. Her proposed research utilizes nanocellulose extracted from lignocellulosic wastes and micro-fibrillar cellulose to develop high-quality bio-based sustainable products. She is passionate about researching the pulping process as she studied in wood and pulp industries for MSc. She will join the ERMP program in June 2023 and she will be responsible for conducting experimental research related to mechanical refining and fractionation of thermo-mechanical pulping processes. In particular, she will identify and formulate relevant problems, choose appropriate tools and develop solutions.

Graduate students

Sam Brown

After completing 3 co-op terms with the team and his undergraduate degree in physics, Sam is joining on as a master's student in mechanical engineering under the supervision of Drs. Mark Martinez and James Olson. In previous work terms, he contributed to Project 3.2 by studying wood compression and co-creating the Pulp and Paper Centre Image Processing Toolbox. In his master's thesis, he will continue the wood compression research and investigate the absorption of water into paper sheets using a variety of imaging techniques

Adam Wu

Dr. Adam (Jie) Wu holds a bachelor's degree (Bachelor of Science, 2015), a master's degree (Master of Engineering Leadership, 2017), and a Doctorate (Doctor of Philosophy, 2021), all obtained from UBC. He is currently a Postdoctoral Researcher co-supervised by Prof. Scott Renneckar and Prof. Jack Saddler. Adam's Ph.D. work focuses on repurposing the mechanical pulping technique into a pretreatment/front-end for an enzyme-based biorefinery process. As a member of the Energy Reduction in Mechanical Pulping (ERMP) research program, Adam's current research goal aims at adding value to the mechanical pulping-derived byproducts (pulp fines), through chemo-enzymatic approaches, with the hope of displacing conventional fossil-based products.

ERMP PERSONNEL UPDATES

Co-op Students

Salman Dajani

Salman was our co-op student for the winter term. Salman is currently pursuing a BASc in Engineering Physics at UBC and worked with us on preparing and testing handsheets as part of Project 1.1. Salman had always been curious about research, so when he saw the role that the Pulp and Paper Centre was offering, he jumped at the opportunity! Salman found it to be a great experience, and he looks forward to pursuing more research roles during his time at UBC.

Stephen Lee

Stephen is returning to ERMP from last summer after having completed his second year of mechanical engineering with a minor in computer science at UBC's Okanagan campus. He will be continuing work on Project 1.1, as well as testing for ongoing projects.

Nicole Ting

Nicole is currently pursuing a Bachelor of Science in Forest Bioeconomy Sciences & Technology at the University of British Columbia. Nicole is a co-op student that is working with Adam and Siwei on Project 2.1. Nicole enjoys gaining hands on lab experience and is interested in the development of pulp and paper products. Prior to joining the ERMP team, Nicole has completed 3 years of studies and 1 co-op work term.

Farah Sadek

Farah is a 3rd-year Chemical and Biological Engineering Student at the University of British Columbia. Over the Summer, Farah will work under Mariana Frias de Albuquerque and Dr. Heather Trajano, researching MFCs and Fines in Mechanical pulping. Outside of the lab, Farah's interests include reading, drawing, disability advocacy, and spending time with friends.

ERMP PERSONNEL UPDATES

Work Learn Student

Nilgun Abali

Nilgun is so excited to be joining ERMP this summer, and will be producing and testing handsheets as part of her role in ERMP. She is currently pursuing a degree in mechanical engineering at the University of British Columbia. Nilgun is eager to learn more about mechanical pulping and is excited to be immersed in this research environment. In her free time, Nilgun enjoys pursuing her hobbies, which include photography, art, cooking, and fitness.

Recent Publications by the ERMP team

1. Ferreira, E. S., Drummond, J., Veiga, A. T., Sibellas, A., Brown, S., Cranston, E. D., & Martinez, D. M. (2023). “Mapping absorbency in cellulosic fibres with iron tracers”. Carbohydrate Polymers, 311, 120785.

2. Ferreira, E. S.; Drummond, J.; Veiga, A. T. V.; Seppänen, T.; Sibellas, A.; Brown, S.; Turpeinen, T.; Martinez, D. M.; Cranston, E. D. (2023). “Enhanced Visualization and Property Mapping of Lightweight and High Bulk Lignocellulosic Materials by Micro-Computed Tomography” American Society Chemistry Spring, Indianapolis. (submitted)

3. Fang, M., Sibellas, A., Drummond, J., Cao, Y., Phillion, A., Martinez, M., Pediredla, V., and Gopaluni, B. (2023). "Deep learning-based hybrid reconstruction algorithm for fibre instance segmentation from 3D X-ray tomographic images." The Canadian Journal of Chemical Engineering. https://doi.org/10.1002/cjce.24939

4. Fang, M., Wattoo, E., Palmer, B., Guliov, D., Bicho, P., Cao, Y., Pediredla, V., Gopaluni, B. “Real-time Process Operation Evaluation and Model Reliability Assessment for Chemi-thermomechanical Pulping Process”. Control Engineering Practice (Under review – Minor revisions).

PPC HIGHLIGHTS

Richard Kerekes 2023 CHBE Hall of Fame Inductee

We would also like to extend our appreciation to our colleague and dear friend, Dr. Richard Kerekes, for his induction into the prestigious 2023 CHBE Hall of Fame at UBC.

"In recognition of his outstanding contributions to the UBC Pulp and Paper Centre, the department and its student body, and the profession of chemical and biological engineering, including his national leadership and seminal research toward fundamental understanding and technology development to improve fibre quality for paper-making.

Dr. Kerekes is widely regarded as one of Canada's most important and influential scholars in the areas of fibre processing and papermaking technology, and is the recipient of the John S. Bates Memorial Gold Medal of the Pulp and Paper Technical Association of Canada and the TAPPI Gunnar Nicholson Gold Medal. In 2018, Dr. Kerekes was inducted into the Paper Industry International Hall of Fame in Appleton, WI."

UBC CHBE 2023 Hall of Fame Inductees: Immy S. H. Lee, Richard Kerekes and Patrick Daniel.

PPC HIGHLIGHTS

Ongoing Research at the PPC Pilot plant

Authors: Michael Bilek, James Olson, Norman Roberts

Michael Bilek has been an active research assistant with the ERMP program for the past three years. His current research focuses on the exploring microfibrillated cellulose (MFC) composite materials. Michael's specific objective is to gain a comprehensive understanding of the MFC composite matrix to predict the mechanical properties of composites, which vary in terms of MFC/long fiber ratios.

To date, we have refined BCTMP aspen to 1500 kWh/t, resulting in the production of 280 L of highly refined MFC. These MFC samples possess a length-weighted average fiber length of 0.16 mm, comprised of 90% fines (within the detection limits of a Fiber Quality Analyzer). We subsequently fractionated the stock BCTMP aspen through a Bauer-McNett fractionator, yielding R28, R48, R100, and R200 fraction. By combining these fiber fractions with varying ratios of MFC, we are able to produce composite handsheets for subsequent mechanical testing, see figures below. These tests will provide insights into how the physical properties of these composites evolve with differing MFC ratios, and enable us to predict the mechanical properties of composite ratios beyond our immediate experimental scope.

Michael is also utilizing imaging techniques such as scanning electron microscopy and micro-computed tomography. These sophisticated imaging methodologies enable a thorough examination of the fiber-fiber bonding mechanisms and overall structure of the MFC composites, facilitating a comprehensive analysis of their composition and architecture.

Mechanical testing and imaging of MFC composites will provide a fundamental insight into how MFC can be better utilized to form novel products with specific mechanical properties.

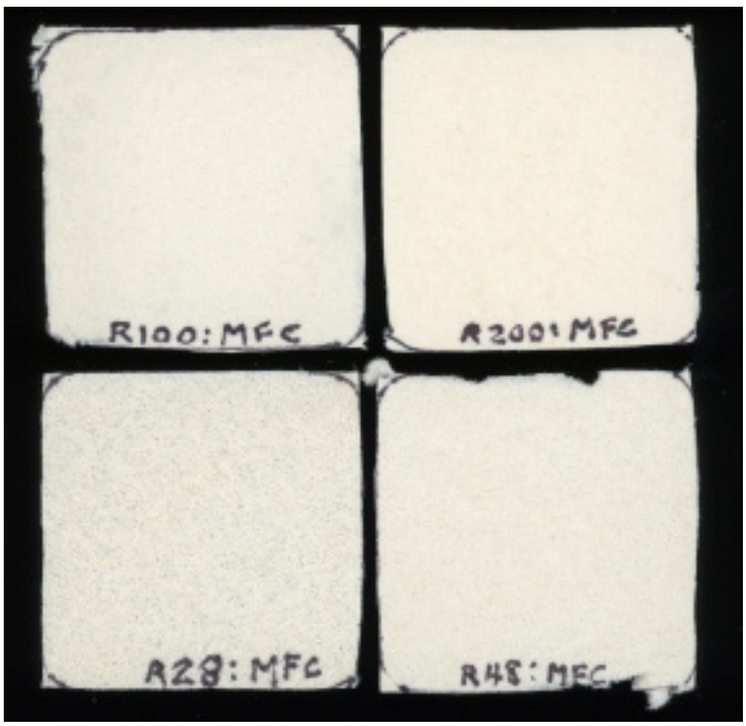

Different composites of MFC and aspen pulp.

Salman, Norm and Michael in the PPC pilot plant.

CONTACTS

You are welcome to contact any of the API Professors:

Mark Martinez
Professor, UBC
604-822-8564
Mark.Martinez@ubc.ca

James Olson
Professor, UBC
604-822-5705
James.Olson@ubc.ca

Rodger Beatson
Professor, BCIT
604-432-8951
Rodger_Beatson@bcit.ca